

# Graph-based Facial Affect Analysis: A Review of Methods, Applications and Challenges

Yang Liu, Xingming Zhang, Jinzhao Zhou, Xin Li, Yante Li, and Guoying Zhao, *Senior Member, IEEE*

**Abstract**—Facial affect analysis (FAA) using visual signals is important in human-computer interaction. Early methods focus on extracting appearance and geometry features associated with human affects, while ignoring the latent semantic information among individual facial changes, leading to limited performance and generalization. Recent work attempts to establish a graph-based representation to model these semantic relationships and develop frameworks to leverage them for various FAA tasks. In this paper, we provide a comprehensive review of graph-based FAA, including the evolution of algorithms and their applications. First, the FAA background knowledge is introduced, especially on the role of the graph. We then discuss approaches that are widely used for graph-based affective representation in literature and show a trend towards graph construction. For the relational reasoning in graph-based FAA, existing studies are categorized according to their usage of traditional methods or deep models, with a special emphasis on the latest graph neural networks. Performance comparisons of the state-of-the-art graph-based FAA methods are also summarized. Finally, we discuss the challenges and potential directions. As far as we know, this is the first survey of graph-based FAA methods. Our findings can serve as a reference for future research in this field.

**Index Terms**—Facial Affect Analysis, Facial Expression Recognition, Micro-expression Recognition, Action Unit Detection, Affective Graph Representation, Graph Neural Network.

## 1 INTRODUCTION

FACIAL affects are one of the most important visual signals for developing human-computer interaction systems, because it conveys critical information that reflects emotional states and reactions in human communications [1, 2, 3]. During the past decade, many facial affect analysis (FAA) methods have been explored benefiting from interdisciplinary studies of affective computing, computer vision and psychology [4, 5, 6]. Some of them have been extended to many applications including medical diagnosis [7], social media [8] and video generation [9]. Meanwhile, competitions such as FERA [10], EmotiW [11], Aff-Wild [12], ABAW [13], EmotioNet [14], AVEC [15] and MuSe [16] are regularly held to evaluate the latest progress and propose frontier research trends.

As early as the 1970s, Ekman and Friesen [17] proposed the definition of six basic affects, i.e., *happiness*, *sadness*, *fear*, *anger*, *disgust*, and *surprise*, based on an assumption of the universality of human affective display [18]. Another kind of popular description, called Facial Action Coding System (FACS), was designed for a wider range of affects, which consists of a set of atomic Action Units (AUs) [19, 20]. Figure 1 shows an example of six basic affects plus *neutral* and activated AUs in each facial affect. Both of the above are categorical models. Besides, other findings suggest a dimensional affective model [21, 22, 23], with valence and arousal (V-A), which is considered more appropriate to

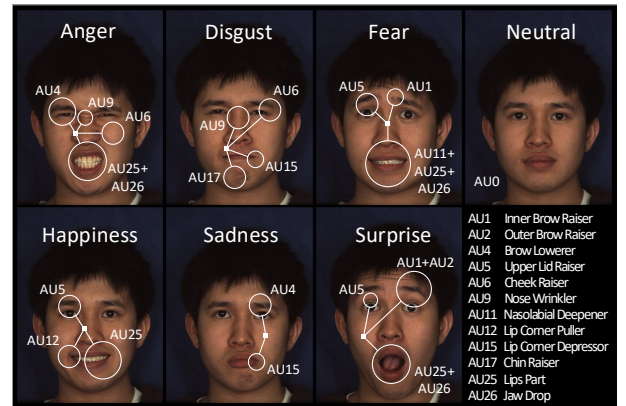


Fig. 1. An example of basic facial affects and related AU marks. AU0 denotes no activated AU. Images are from BU-4DFFE [26] database.

describe dynamic changes of human affects in real-world [24, 25].

Historically, FAA methods have undergone a series of evolutions. Initial studies usually rely on hand-crafted design or classic machine learning to obtain useful affective features without structural information [5, 27]. Psychological findings indicate that the human cognition of facial information is realized through a dual system composed of analytic processing and holistic processing [2]. The former acquires multi-dimensional cluster features by analyzing local facial areas, while the latter aims to generate a holistic representation to perceive the overall structure [2, 19]. A reasonable idea for machine vision researchers is to model this topology-like working system. Accordingly, many state-of-the-art studies have been dedicated to generate a facial graph with local-to-global affective features [28, 29, 30, 31].

If the above evidence reveals the feasibility of using graph-based methods for FAA, researches on how facial

- Y. Liu, X. Zhang and J. Zhou are with the School of Computer Science and Engineering, South China University of Technology, Guangzhou 510006, China. E-mail: liuy17@163.com, cszxm@scut.edu.cn, charlesmzhouscut@gmail.com.
- X. Li is with the Department of Electrical and Computer Engineering, Rutgers University, Piscataway, NJ-08854, United States. E-mail: xin.li.ece@rutgers.edu
- Y. Liu, Y. Li and G. Zhao are with the Center for Machine Vision and Signal Analysis, University of Oulu, Oulu, FI-90014, Finland. E-mail: {firstname.lastname}@oulu.fi

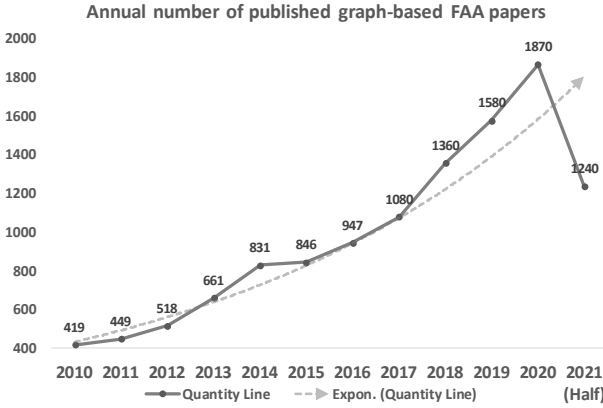


Fig. 2. The growth trend of papers related to graph-based FAA.

muscles participate in affective expression further demonstrate its possibility as a necessary condition [18, 32, 33]. There are latent relationships (also known as AU dependencies in FACS) among different facial areas and contexts, which are proved to be important clues [20, 34]. A few non-graph-based deep models have partly captured these relationships and achieved performance improvement [35, 36, 37]. The underlying assumption is that explicit mappings which reflect this kind of relationship can be directly learned [38]. However, in real-world, these mappings are not solid enough, because they differ from subject to subject and even from one condition to another [39, 40]. Recently, graph-based methods have shown their ability to represent facial anatomy and simultaneously fit latent relationships in facial affects [41, 42, 43]. Some pilot studies have also suggested that the graph-based method can even move beyond to deal with challenging tasks such as analyzing occluded face [44, 45] and ambiguous facial affects [46, 47].

By searching on Google Scholar using keywords of ‘graph’ and **Index Terms** in this survey, we have counted the number of relevant published papers from 2010 to the present. As presented in Fig. 2, the graph-based FAA method has gained increasing attention, especially in the past five years (over 1,200 papers have been published in the first half of 2021).

In this work, we review the state of FAA research using graph-based methods. Despite there have been many reviews that discussed historical evolutions [5, 38, 48] and recent advances [25, 49, 50] of FAA, including some on specific problems like occlusion expression [51], multi-modal affect [52] and micro-expression [53]. This is the first systematic and in-depth survey for the graph-based FAA field, as far as we know. We emphasize representative researches proposed after 2010. The goal is to present a novel perspective on FAA and its latest trends.

This review is organized as follows: Section 2 introduces a generic pipeline of FAA and briefly discusses facial preprocessing methods. Section 3 presents a taxonomy of mainstream graph-based methods for affective representation. Section 4 reviews traditional and advanced approaches for graph relational reasoning and discusses their pros and cons in FAA tasks. In Section 5, we summarize public databases, main FAA applications, and current challenges based on a detailed comparison of related literature. Finally, Section 6 concludes with a general discussion and identifies potential directions.

## 2 FACIAL AFFECT ANALYSIS

### 2.1 General Pipeline

A standard FAA method can be broken down into fundamental components: face preprocessing, affective representation and task analysis. As a new branch of FAA, the graph-based method also follows this generic pipeline (see Fig. 4). Face detection and registration are two necessary pre-steps that first locate faces and normalize facial variations, sometimes also provide facial landmarks [54, 55]. Figure 3 presents an illustration of the preprocessing steps. Early methods like *Viola and Jones* [56], *Mixtures of Trees* [57], and *Active Appearance Model (AAM)* [58] have been widely used for this purpose. Recently, cascaded deep approaches with real-time performance are popular, such as *Multi-Task Cascaded Convolutional Network* [59], *Hyperface* [60], and *Supervision by Registration and Triangulation* [61]. For more specific information, please refer to [62, 63, 64].



Fig. 3. An illustration of face detection and face registration. The happy image is from CK+ database [65].

Comparing to other existing methods, the graph-based FAA pays more attention to how to represent facial affects with graphs and how to obtain affective features from such representation by graph reasoning. Naturally, depending on different affective graph representations, generic approaches need to be adjusted or new graph-based approaches should be proposed to infer the latent relationship and extract the final affective feature. The two components can either be performed separately or arranged as an end-to-end framework. Hence, the advantages and limitations of different graph generation methods and their relational reasoning approaches are two main topics of this survey.

### 2.2 Role of Graph

As mentioned above, it is meaningful to use graphs to represent and analyze the structural information in facial affects. In mathematical terms, a graph can be denoted as  $G = (V, E)$ , where the node set  $V$  contains all the representation of the entities in the graph and the edge set  $E$  contains all the relations between two entities.  $E$  is often represented as an adjacency matrix  $A$  where each element  $A_{ij}$  attributes for a degree of relation between the node  $N_i$  and  $N_j$ .  $V$  is represented as the feature matrix  $H$  where each vector  $H_i$  denotes the feature representation of a node  $N_i$ .

Obviously, all the structure information of a graph is contained in  $E$ . Thus, when  $E$  is empty,  $G$  becomes an unstructured collection of entities (i.e., independent local facial areas [35]). Given this unstructured collection, performing relational reasoning requires the model to infer the structure of these entities at a higher-order before predicting the property or category of an object. Meanwhile, we could also define some initial graph structure ahead of the relational model, which is a general practice in many affective graph representations [31, 44, 66]. With richer information

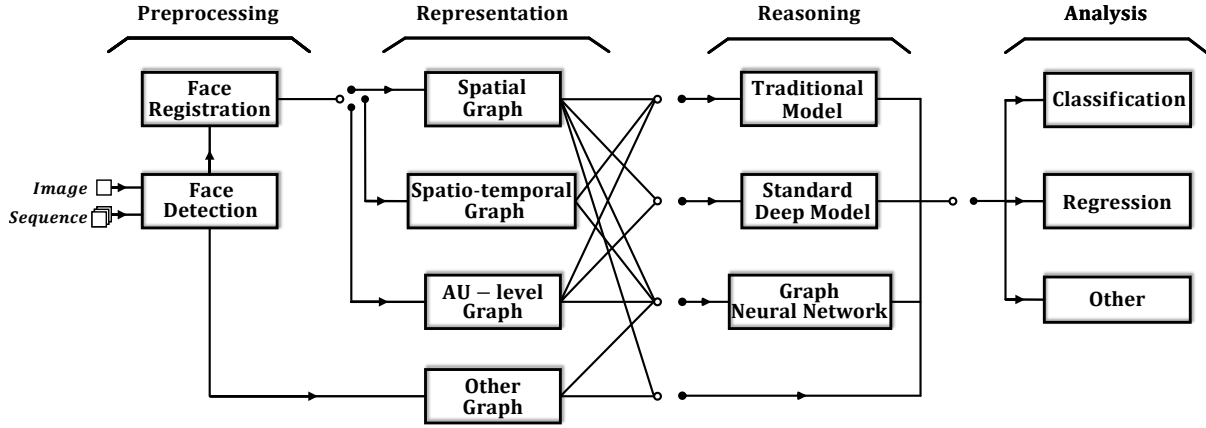


Fig. 4. The pipeline of graph-based facial affect analysis methods.

being manually or automatically provided through prior knowledge, the graph-based FAA methods are expected to exhibit better performance and generalization capability.

### 3 GRAPH-BASED AFFECTIVE REPRESENTATIONS

Affective representation is a crucial procedure for most graph-based FAA methods. Depending on the domain that an affective graph models, we categorize the strategy as spatial graph, spatio-temporal graph, AU-level graph and others. Figure 6 illustrates a detailed summary of the literature using different graph representations. Note that many graph-based representations contain pre-extracted geometric or/and appearance features. Whether it is hand-crafted or learned, these feature descriptors are not essentially different from those used in non-graph-based affective representations. Interested readers can refer to [5, 48, 49] for a systematic understanding of this topic.

#### 3.1 Spatial Graph Representations

Spatial representations aim to encode geometry or appearance from an affective face. Generic spatial methods treat a facial affect as a whole representation or pay attention to variations among main face components or crucial facial parts [35, 67, 68]. For graph-based spatial representations, not only facial changes are considered, but also their co-occurring relationships and affective semantics are regarded as important cues [28, 69, 70]. The approaches used to generate spatial affective graphs can be divided into landmark-level graphs and region-level graphs. Figure 7 illustrates frameworks of different spatial graph representations.

##### 3.1.1 Landmark-level graphs

Facial landmarks are one of the most important geometry that reflects the shape of face components and the structure of facial anatomy. An illustration is shown in Fig. 5. Thus, it is a natural idea to use facial landmarks as base nodes for generating a graph representation. Note that facial shape is not the only information that landmark-level graphs encode, facial appearances like color [71] and texture [72] are also exploited to enrich landmark-level graphs.

Limited by the performance of landmark detection algorithms, only a few landmarks are applied in early graph representations [73, 74], which describe the geometric information attached to basic face components. Recently, graph representations using more facial landmarks are proposed to depict fine-grained facial shapes [75]. The 68 landmarks

detected by *dlib* library [76] or the 66 landmarks provided by AAM are also widely used in the graph construction. For example, in [40] and [77], the authors associated the 68 landmarks with the AUs in FACS and made graph-based representations. The difference is that the former additionally employed local appearance features extracted by *Histograms of Oriented Gradients (HOG)* [78, 79] as attributes of nodes, while the latter proposed two strategies, *full-face graph* and *FACS-based graph*, for enhanced geometric representations. Specially, [80] formulated a *Latent Tree (LT)* where 66 landmarks were set as part of leaf nodes accompanied by several other leaf nodes of AU targets and hidden variables. This graphical model represented the joint distribution of targets and features that was further revised through conducting graph-edits for final representation.

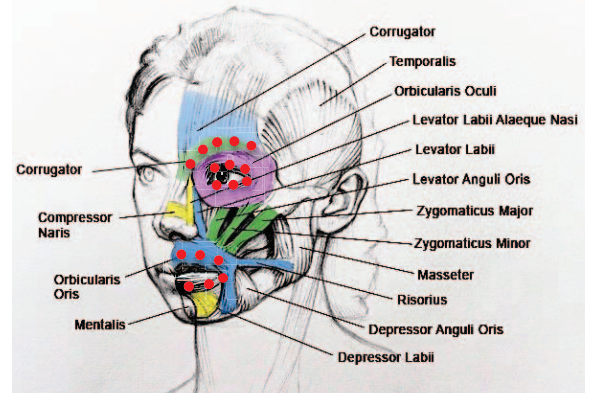
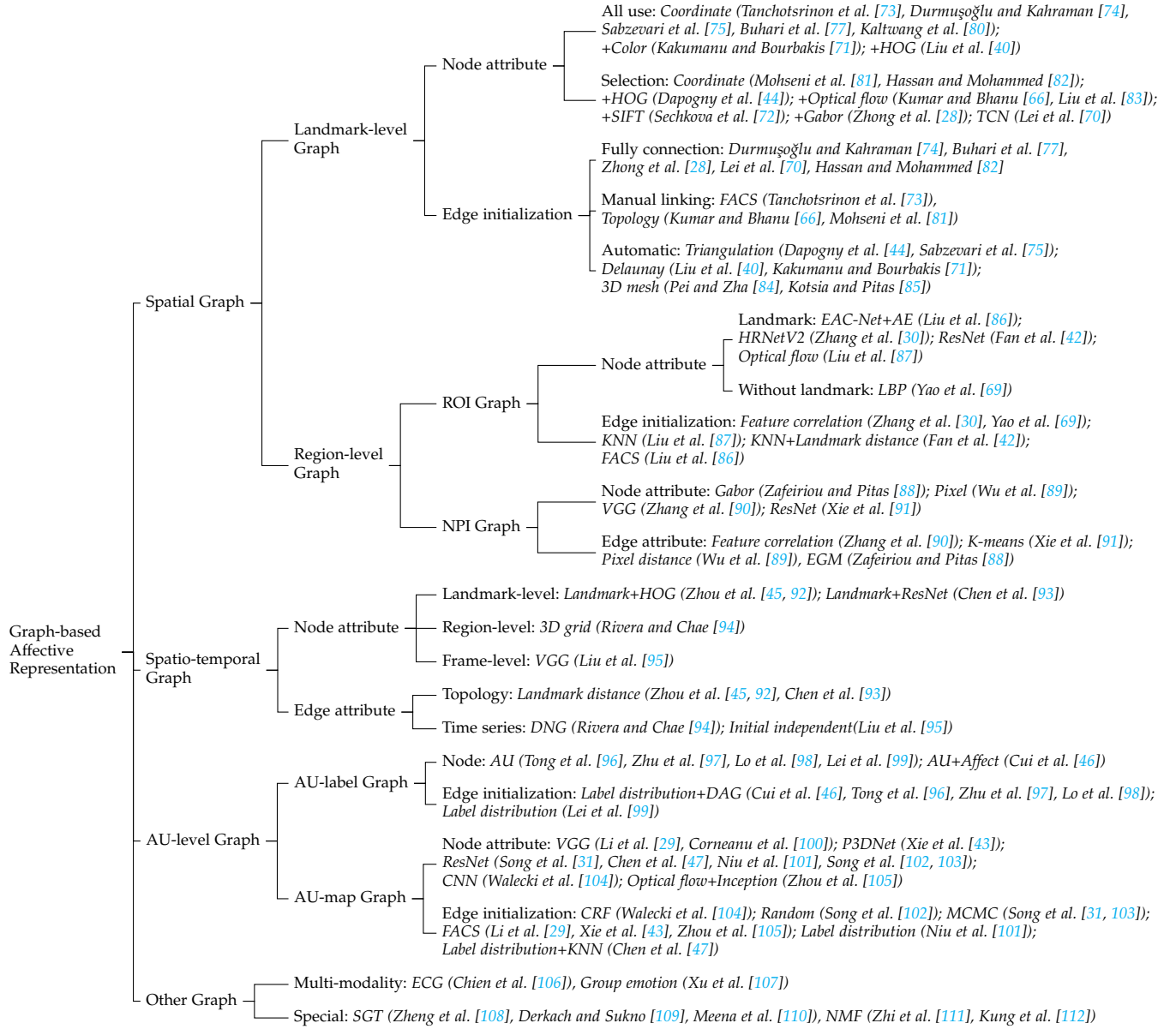


Fig. 5. Facial muscle anatomy and related landmarks [81].

Furthermore, some current methods select landmarks with significant contributions to avoid redundant information [70, 82]. Landmarks locating external contour and nose are frequently discarded [44, 81] (see Figs. 7a, 7b), because they are considered irrelevant to facial affects. [72] and [28] chose to remove the landmarks of the facial outline and applied a small window around each remaining landmark as one graph node, while the local features were extracted by *Scale Invariant Feature Transform (SIFT)* [113] and *Gabor filter* [114], respectively. As mentioned at the beginning, since these local areas were segmented to introduce facial appearance into the graph representation rather than as independent nodes, similar to [40], these methods are still classified in landmark-level graphs. On the other hand, strategies of adding extra reasonable landmarks have been designed to generate comprehensive graph representations



Fig. 6. Taxonomy for Graph-based Facial Representation.



[66, 115], which could keep an appropriate dimension and represent more sufficient affective information.

For edges in landmark-level graphs, a fully connected graph is the most intuitive way to form edges [28, 70, 74, 77, 82]. However, the number of edges is  $n(n-1)/2$  for a complete graph with  $n$  nodes, which means the complexity of the spatial relationship will increase as the number of nodes increases. This positive correlation is not so correct in analyzing facial affects. For example, assuming the left eyebrow has five landmarks (see Fig. 5), the edge connecting adjacent landmarks or landmarks at both ends is obviously helpful. By contrast, links between other non-adjacent nodes seem not that necessary. Since the various parts of the eyebrow mostly move in concert when displaying facial affects, the changing trends contained in these edges are redundant. To this end, researches like [66, 73, 81, 115] manually reduced edges based on knowledge of muscle anatomy and FACS. Another type of approaches is to exploit triangulation algorithms [44, 75], such as *Delaunay* triangulation [71], to generate edges of a facial graph. The triangular patches

formed by landmarks are consistent with true facial muscle distribution and edges are uniform for different subjects [40]. Similarly, the landmark-level graph with triangulation is also utilized in generating a sparse or dense facial mesh for 3D FAA [84, 85]. For edge attributes of the above facial graphs, the *Euclidean* distance is the simplest and most dominant metric, even with multiple normalization methods including diagonal line [73], inner-eyes distance [40] and maximum distance [82]. The gradient computation [77] and *Hop* distance [92] have also been explored as edge attributes to model spatial relationship in different levels. Apart from these strategies, several learning-based edge generation methods (e.g., *Bayesian* method [75], *LT* [80], *Conditional Random Field* (CRF) [104]) have been proposed to automatically extract semantic information from facial graphs. This part is discussed in detail in Sec. 4.1 and 4.4.

### 3.1.2 Region-level graphs

Region-level representations usually describe faces in terms of individual local areas and thereby ignore the spatial rela-

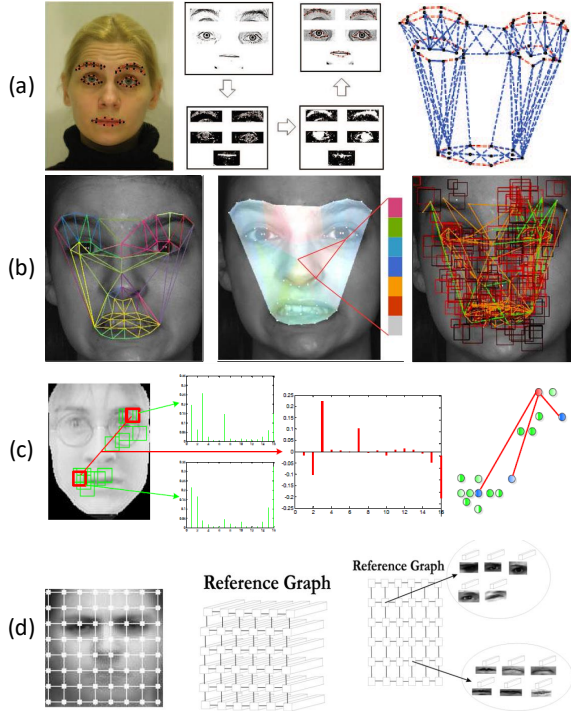


Fig. 7. Spatial graphs. (a) Landmark-level graph with FACS-based edges [81]; (b) Landmark-level graph with automatic triangle edges [44]; (c) ROI graph with edges computed based on correlation [69]; (d) NPI graph with individual nodes [88]. Zoom in for better view.

tionships among facial components. To solve this shortcoming, using graph structure to encode the spatial relations into the region-level representation is intuitive. There are two categories of region-level affective graphs: region of interest (ROI) graphs and non-prior information (NPI) graphs.

ROI graphs partition a set of facial areas as graph nodes which are highly related to affective display. Coordinates of facial landmarks are commonly applied to locate and segment ROIs. Unlike a few landmark-level graphs that only use texture near all landmarks as supplementary information, ROI graphs explicitly select meaningful areas as graph nodes, and edges do not entirely depend on established landmark relationships. [30] employed the *High-Resolution Network (HRNetV2)* [116] to regress ROI maps spotted by representative landmarks. Each spatial location in the extracted feature map was considered as one graph node, while edges were induced among node pairs according to mappings between ROIs and AUs. Another example in [42] utilized feature maps of landmark-based ROIs outputted by the *ResNet50* [117] as nodes to construct a *K-Nearest-Neighbor (KNN)* graph. For each node, its pair-wise semantic similarities were calculated, and the nodes with the closest *Euclidean* distance were connected as initial edges. Similarly, [87] also employed landmark-based ROIs, but the *KNN* graph was generated in *optical-flow* space to encode the local manifold structure for a sparse representation [83]. Due to different AUs possibly occurring at the same location, [86] firstly defined both local and global ROIs by taking FACS and landmarks as references, which subsequently refined by the *Enhancing and Cropping Network (EAC-Net)* [118]. Each ROI was then fed into an *Auto-Encoder (AE)* for node attributes. In addition, the method of obtaining ROIs without relying on facial landmarks has also been studied. [69] proposed a pair-wise learning strategy to automatically discover re-

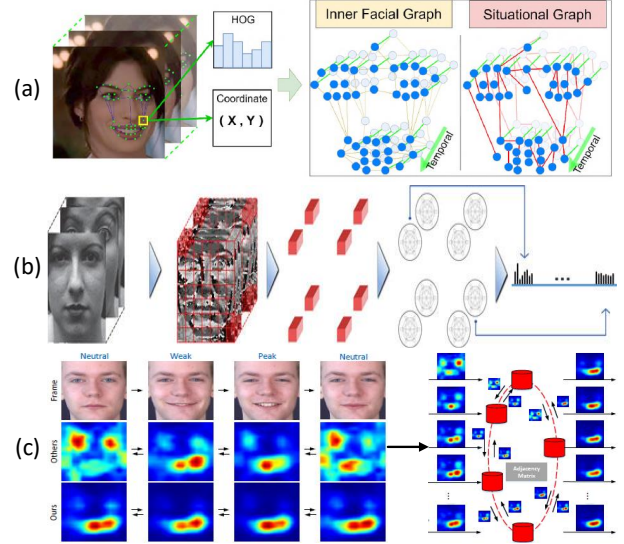


Fig. 8. Spatio-temporal graphs. (a) Landmark-level graph with adaptive edges [45]; (b) Region-level graph with edges based on transitional masks [94]; (c) Frame-level graph [95]. Zoom in for better view.

gions that were in part consistent with the locations of AUs (see Fig. 7c). The *Local Binary Pattern (LBP)* histograms [27] of the learned ROIs and their feature correlations were taken as node and edge attributes of an undirected graph (either fully connected or highly sparse), respectively.

Different from ROI graph representations, nodes in NPI graphs are evenly distributed in raw images or generated in a fully automatic manner without external knowledge. [88] created a reference bunch graph by evenly overlaying a rectangular graph on object images (see Fig. 7d). For each node of the graph, *Gabor* filters [119] was utilized to compute a set of feature vectors for different facial instances. The graph structure was optimized by solving an *Elastic Graph Matching (EGM)* problem which is discussed in Sec. 4.4. Such grid-derived graph representation was also applied in [89]. Recently, several methods try to introduce regions beyond facial parts or single face images as context nodes. [90] exploited the *Region Proposal Network (RPN)* [120] with *VGG16* [121] to extract regions-level nodes including both the target face and its contexts, while edges were affective relationships calculated based on feature vectors. [91] built two NPI graphs for cross-domain FAA. Holistic and local feature maps were firstly extracted from corresponding regions by *ResNet50* [122] for both the source and the target domain. Then, three types of connections, global-to-global connection, global-to-local connection, and local-to-local connection were computed according to statistical feature distribution acquired by *K-means* algorithm and fine-grained iterative update.

### 3.2 Spatio-Temporal Graph Representations

Literally, spatio-temporal representations deal with a sequence of frames within a temporal window and describe the dynamic evolution of facial variations. In particular, introducing temporal information allows nodes at different times to interact with each other, and generates a more complex affective graph. Figure 8 presents frameworks of different spatio-temporal graph representations.

Extend spatial graphs to the spatio-temporal domain is currently the main route. [94] exploited a *Kirsch* compass mask [123] and a *Gaussian-like* weighted compass mask to

obtain 2D directional number responses and 3D space-time directional edge responses corresponding to each of the symmetry planes of a cube. The two masks of given local neighborhoods were nodes in a spatio-temporal *Directional Number Transitional Graph (DNG)*, which could represent salient facial changes and statistic frequency of affective behaviors over time (see Fig. 8b). Several representations have been proposed to define temporal connections between landmarks, which can be seen as landmark-level spatio-temporal graphs. [92] developed a spatial temporal facial graph where intra-face edges were initialized based on semantic facial structure and inter-frame edges were created by linking the same node between consecutive frames. Similar landmark-based edge initialization in the temporal domain was also utilized in [93]. In [45], authors introduced a connectivity inference block that could automatically generate dynamic edges for a spatio-temporal situational graph of part-occluded affective faces (see Fig. 8a). Unlike landmark-level graphs, [95] first extracted a holistic feature of each frame and set them as individual nodes to establish a fully connected graph (see Fig. 8c). The edge connections would be updated during learning long-term dependency of nodes in time series, which could be seen as a frame-level spatio-temporal graph.

### 3.3 AU-level Graph Representations

Apart from using knowledge of AUs and FACS in the above two types of affective graphs, many graph-based representations have been proposed to model affective information from the perspective of AUs themselves. We divide these approaches into two categories: AU-label graph and AU-map graph. Figure 9 shows frameworks of different AU-level graph representations.

#### 3.3.1 AU-label graphs

Different from spatial and spatio-temporal graphs, AU-label graphs were built from the label distribution of training data [41, 97]. [96] computed the co-occurrence and co-absence dependency between every two AUs from existing database (see Fig. 9a). Since the dependency is not always symmetric, these AU label relationships were used as edges to construct a *Directed Acyclic Graph (DAG)*. In [98], an AU-label graph was built with a data-driven asymmetrical adjacency matrix that denoted the conditional probability of co-occurring AU pairs. Although the edge initialization was similar, [99] transformed AU labels into high-dimensional node vectors by *Word Embedding* [124] to replace the *one-hot* code in [98]. On the other hand, [46] established a *DAG* where object-level labels (facial affect category) and property-level labels (AU) were regarded as parent nodes and child nodes, respectively. The conditional probability distribution of each node to its parents was measured to obtain graph edges for correcting existing labels and generating unknown labels. Similar idea was also achieved in [47] to boost affective feature learning in large-scale FAA databases (see Fig. 9c).

#### 3.3.2 AU-map graphs

AU-map graphs are intuitively close to region-level spatial graphs, especially ROI graphs because they both employ local feature maps as graph nodes. [29] is an example in between. Twelve AUs features were learned through landmark-based ROI features cropped from a multi-scale

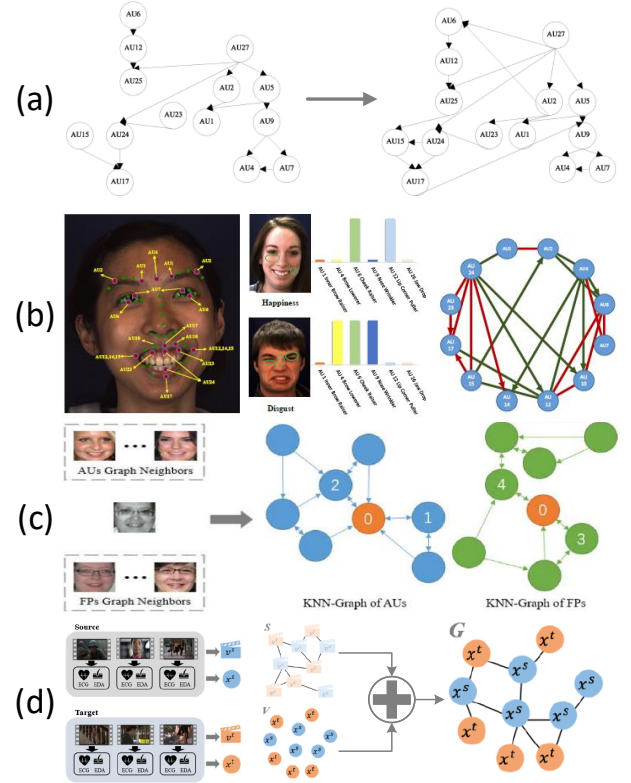


Fig. 9. AU-level and Multi-modal graph representations. (a) AU-label graph with edges generated from training data [96]; (b) AU-map graph with FACS based edges [29]; (c) Auxiliary graphs of both AUs and landmarks [47]; (d) Multi-modal graph of both visual and physiological signals [106]. Zoom in for better view.

global appearance feature [121]. These AU features and the AU relationships gathered from both training data and manually pre-defined edge connections [125] were combined to construct a knowledge graph (see Fig. 9b). However, the significant difference is that AUs define a set of facial muscle actions, which means there might be multiple AUs in the same ROI. Like in Fig. 1, both AU12 and AU15 occur at lip corners but refer to ‘puller’ and ‘depressor’, respectively. Therefore, for many AU graphs, their definition of nodes is independent of those in ROI graphs, even though they are similar in feature map extraction. For instance, graph nodes in [43] were AU features directly obtained by a *Pseudo-3D Residual Network (P3DNet)* [126] without defining ROIs. The homologous protocol was also conducted in [105] and [103].

Some special AU-map graphs have been proposed to introduce structure learning for more complex FAA tasks. For AU intensity estimation, [104] trained a *Convolutional Neural Network (CNN)* to jointly learn deep AU features from multiple databases. The *copula functions* [127] was applied to model pair-wise AU dependencies in a CRF graph. In addition, *Bayesian network (BNs)* are also used to capture the AU inherent dependencies for this task [31, 103]. To account for indistinguishable affective faces, [100] designed a VGG-like patch prediction module plus a fusion module to predict the probability of each AU. A prior knowledge taken from the given databases and a mutual gating strategy were used simultaneously to generate initial edge connections. To model uncertainty samples in real-world databases, [102] established an uncertain graph, in which a weighted probabilistic mask that followed *Gaussian* distribution was imposed on each AU feature map. By doing this, both the importance



of edges and the underlying uncertain information could be encoded in the graph representation. Another attempt in [101] boosted semi-supervised AU recognition for both labeled and unlabeled face images. The parameters of two AU classifiers were used as graph nodes to share the latent relationships among AUs.

### 3.4 Other Representations

Recently, several graph representations that do not fall into the above categories have been proposed, which indicates that this is still an open research field. To combine signals from multiple corpora, [106] proposed a dual-branch framework, in which the visual semantic features were extracted by a 3DCNN [128] in both source and target sets. These features were then retrieved with correlation coefficients to generate positive edge connections for a learnable visual semantic graph (see Fig. 9d). Besides, [107] built an emotion-based directed graph according to label distributions of facial affects in existing training data. Specifically, its nodes were initialized word vectors of the corresponding affects, while the edges represented conditional probabilities of pair-wise affects. The learned local relationship patterns could be injected into a network at the feature level to enhance the performance of final multimedia affect tagging.

In addition, some special graph representations of FAA such as *Spectral Graph Transform (SGT)* [108, 109, 110] and *Non-negative Matrix Factorization (NMF)* [111, 112] have also been explored.

### 3.5 Discussion

As an important part of graph-based FAA, there is a certain causal relationship between the choice of graph representation methods and the selection of relational reasoning methods. The spatio-temporal graph and the AU-level graph are the most notable recent trends of graph-based facial representations. The limitations of the three types are discussed as follows.

*Spatial graph representations:* Conceptually, landmark-level graphs have certain limitations both externally and internally. On one hand, most of the generated graphs are sensitive to detection errors of facial landmarks, thereby may fail in uncontrolled conditions. On the other hand, the selection of landmarks and the connection of edges have not yet formed a standard rule. Although some FACS-based strategies have been designed, the effects of different landmark sets and different edge connections on the graph representation are rarely reported. Finally, the recent trend of developing FAA methods is to combine every procedure as an end-to-end learning pipeline. Thus, how to integrate the process of establishing landmark-level graphs into existing frameworks still needs to be studied.

Comparing with landmark-level graphs by modeling the facial shape variations of fiducial points, region-level graph representations explicitly encode the appearance information in local areas. The spatial relationships among selected regions are measured through feature similarity instead of manual initialization based on facial geometry. The graph reasoning will be the next step to learn task-specific edge connections and discriminative affective features using techniques such as CNNs [129] or *Graph Neural Networks (GNNs)* [130], which are discussed in Sec. 4. The two types of region-level graphs have their own characteristics but have

some flaws as well. For the ROI graphs, the circumstance resulting from inaccurate or unreasonable landmarks will also have an impact on some related representations. In addition, the contribution of geometric information for FAA has been proven in [35], thereby should be more effectively integrated into ROI graph representations. For NPI graphs, incorporating context regions or multiple face regions into graph nodes is an emerging topic. Due to that most existing approaches utilize a region searching strategy, the problem is how to avoid the loss of target face and how to exclude invalid regions. Besides, as far as the literature we have collected, there is no work on combining the ROI graph and NPI graph to construct a joint graph representation, which we think is a promising direction.

*Spatio-temporal graph representations:* Despite the advantage of extra dynamic affective information in spatio-temporal graphs, there are several drawbacks in existing methods. For landmark-level graphs, the current initialization strategy of edge connections is simply to link the facial landmark with the same index frame by frame. No research has been reported to learn the interaction of landmarks with different indexes in the temporal dimension. Besides, in addition to *Euclidean* distance and *Hop* distance, other edge attributes measurement methods should also be explored to model the semantic context both spatially and temporally. For the frame-level graph, the domain knowledge related to affective behaviors like the muscular activity that can be embedded with graph structure is not explicitly considered in recent work. Therefore, building a hybrid spatio-temporal graph is a practical way to encode the two levels of affective information at the same time.

*AU-level graph representations:* Most AU-label graphs rely on the label distributions of one or multiple given databases. One problem is the available AU labels because not every public database provides the annotated AU label. In addition, since AU labeling requires annotators with professional certificates and is a time-consuming task, existing databases with AU annotations are usually small-scale. Therefore, the distribution from limited samples may not reflect the true dependencies of individual AUs. To address this demand, some semi-supervised methods are introduced based on underlying assumptions like the potential mapping between facial affect categories and AUs. However, the reliability of this hypothesis is questionable when faced with complex FAA tasks including micro-expression recognition and continuous affect prediction. Another problem is that the measurement criteria of AU correlations are versatile but not general for both AU-label graphs and AU-map graphs, and can result in different initialized AU dependencies. The impact of these measurements on FAA still needs to be evaluated.

## 4 AFFECTIVE GRAPH RELATIONAL REASONING

Generally, graph relational reasoning is believed to be the crucial step towards actual intelligence [131]. Such a mechanism can be considered as a two-step process, i.e., understanding the structure from a certain group of entities and making inferences of the system as a whole or the property within.

However, things are slightly different in the case of graph-based FAA. Depending on what kind of affective

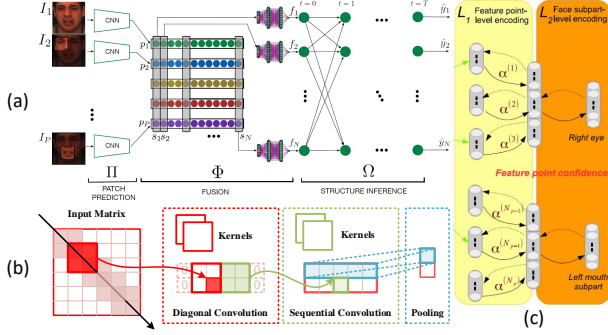


Fig. 10. Classical deep models for graph relational reasoning. (a) RNN [100]; (b) CNN [40]; (c) AE [44]. Zoom in for better view.

graph representation is exploited, the contribution of graph relational reasoning can be either merged before the decision level with other affective features or reflected as a collaborative way in the level of feature learning.

In this Section, we review relational reasoning methods designed for affective graph representations in four categories: *Dynamic BNs (DBNs)*, classical deep models, *GNNs* and other traditional machine learning techniques.

#### 4.1 Dynamic Bayesian Network

*DBNs* are models used to capture relationships mostly in AU-label graph representations. The *BN* is a *DAG* that reflects a joint probability distribution among a set of variables. In this *DAG*, the nodes indicate variables and the edges represent the conditional dependency among variables. In the work of [41, 96], a *DAG* was manually initialized according to prior knowledge, then larger databases were used to perform structure learning to find the optimal probability graph structure. After that, the probabilities of different AUs were inferred by learning the *DBN*. Following this idea, [97] additionally integrated *DBN* to a multi-task feature learning framework and made the AU inference by calculating the joint probability of each category node. Sometimes *DBN* is also combined with some statistical methods to explore different graph structures [31, 103], such as *Monte Carlo Markov Chain* [132] and *Metropolis Hasting algorithm* [133]. Another advanced research of *DBN* is [46]. The inherent relationships between category labels and property labels were modeled by a *DBN*. The *DBN* parameters were utilized to denote the conditional probability distribution of each AU given the facial affect. The wrong labels could be corrected by leveraging the dependencies after the structure optimization.

#### 4.2 Adjustments of Classical Deep Model

Before *GNNs* are widely employed, many studies have adopted conventional deep models to process affective representations with the graph structure. These deep models are not specifically designed but is able to conduct standard operations on graph structural data by adjusting the internal architecture or applying an additional transformation to the input graph representation. Figure 10 shows examples of classical deep models for graph relational reasoning.

##### 4.2.1 Recurrent neural network

The variant of *Recurrent Neural Networks (RNNs)* is one of the successfully extended model types for handling graph structural inputs. Similar to random walk, [28] applied a *Bidirectional Recurrent Neural Network (BRNN)* to deal with

its landmark-level spatial graph representation in a rigid order. To incorporate the structural information represented by *Euclidean* distance, the extracted *Gabor* feature of each node in the graph was updated by multiplying with the average of the connected edges. Subsequently, the nodes were iterated by a *BRNN* with learnable parameters in both the forward and the backward direction. The outputs were further fed to a *fully-connected (FC)* layer and a *softmax* layer for facial affect classification. In the work of [100], the authors built a structure inference module to capture AU relationships from an AU-map graph representation. Based on a collection of interconnected recurrent structure inference units and a parameter sharing *RNN*, the mutual relationship between two nodes could be updated by replicating an iterative message passing mechanism with the control of a gating strategy (see Fig. 10a). The final messages and previous individual AU estimations were combined to produce advanced AU predictions.

##### 4.2.2 Convolutional neural network

Different from the sequential networks, [40] utilized a variant *CNN* to process the landmark-level spatial affective graph. Compared to standard convolution architectures, the convolution layer in this study convolved over the diagonal of a special adjacency matrix so that the information can be aggregated from multiple nodes. Then a list of the diagonal convolution outputs was further processed by three sequential convolution layers which were 1D convolutions. The corresponding pooling processes were performed behind convolution operations to integrate feature sets (see Fig. 10b). Predictions of facial affects were outputted by *FC* and *softmax* layers. Another attempt for landmark-level spatial graph representations is the *Graph Temporal Convolutional Networks (Graph-TCN)* [70]. It followed the idea of *TCNs* that consisted of residual convolution, dilated causal convolution and weight normalization [134]. By using different dilation factors, *TCNs* were applied to convolve the elements that are both inside one node sequence and from multiple node sequences. Thus, the *TCN* for a node and *TCN* for an edge could be trained respectively to extract node feature and edge feature at the same time. Besides, [42] exploited a *Semantic Correspondence Convolution* module to model the correlation among its region-level spatial graph. Based on an assumption that the channels of co-occurring AUs might be activated simultaneously, the *Dynamic Graph Convolutional Neural Network (DG-CNN)* [135] was applied on the edges of the constructed *KNN* graph to connect feature maps sharing similar visual patterns. After the aggregation function, affective features were obtained to estimate AU intensities.

##### 4.2.3 Auto-Encoder network

The approach of *AEs* has also been explored. [44] employed a hierarchical auto-encoder network to capture the relationship from the constructed landmark-level spatial graph. Specifically, the first stage learned the texture variations based on the extracted *HOG* features for each node. While the second stage accumulated features of multiple nodes whose appearance changes were closely related and computed the confidence scores as the triangle-wise weights over edges (see Fig. 10c). Finally, a *Random Forest (RF)* was used for facial affect classification and AU detection simultaneously.



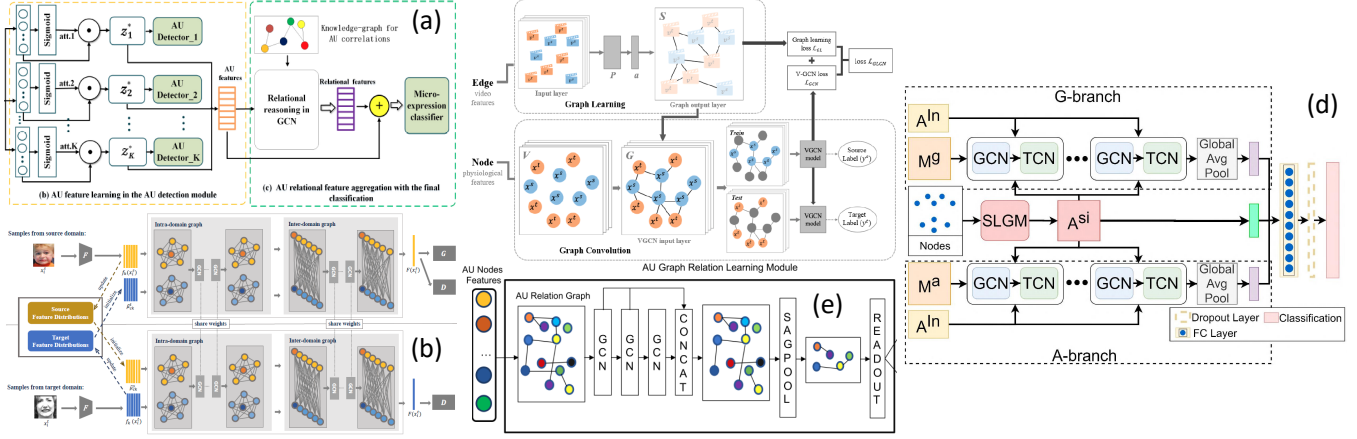


Fig. 11. GNNs for graph relational reasoning. (a) GCN as auxiliary module [105]; (b) GCN for atypical graph representation [91]; (c) GCN as collaborative framework [106]; (d) GCN for spatio-temporal graph representation [45]; (e) GAT [43]. Zoom in for better view.

### 4.3 Graph Neural Network

Not like conventional deep learning frameworks mentioned in Sec. 4.2, GNNs are proposed to extend the ‘depth’ from 2D image to graph structure and established an end-to-end learning framework instead of additional architecture adjustment or data transformation. Several types of GNNs have been successfully used to address the relational reasoning of affective graph representations in FAA methods. Figure 11 illustrates several GNN architectures for graph relational reasoning.

#### 4.3.1 Graph convolutional network

*Graph Convolutional Networks (GCNs)*, especially the spatial GCN [136], are the most popular GNN in graph-based FAA research. Practically, GCNs can be set as an auxiliary module [99] or part of the collaborative feature learning framework [31]. For the former, GCNs are applied immediately after the graph representation. However, the outputs of relational reasoning are not directly used for facial affect classification but are later combined with other deep features as a weighting factor. In [98], the AU relationships were modeled by the conditional probability in an AU-label graph representation. Each one-hot vector of AU labels was fed into a GCN to perform node dependency learning. The generated graph features were embedded to the sequence level deep feature [137] together for final classification. Similarly, [101] employed a two-layer GCN for message passing among different nodes in its AU-level graph. Both the dependency of positive and negative samples were considered and used to infer a link condition between any two nodes. The output of GCN was formulated as a weight matrix of the pre-trained AU classifiers. [105] performed relational reasoning with GCN that provided an updated relational graph feature for each graph node by aggregating features from all neighbors based on edge weights (see Fig. 11a). Besides, GCNs can also be utilized following the above manner to execute relational reasoning on atypical graph representations, such as multi-target graph [90], cross-domain graph [91] (see Fig. 11b) and distribution graph [138].

For the collaborative framework, GCNs usually inherit the previous node feature learning model progressively. Like in [86], a GCN-based multi-label encoder was proposed to update features of each node over a region-level spatial

graph representation. The reasoning process was the same as that in the auxiliary framework. Similar studies also include [30] and [106] (see Fig. 11c). In addition, to incorporate the dynamic in spatio-temporal graphs, [95] set GCNs as an imitation of attention mechanism or weighting mechanism to share the most contributing features to explore the dependencies among frames. After training, the structure helped nodes update features based on messages from the peak frame and emphasize the concerned facial region. A more feasible way is to apply *Spatial Temporal GCN (STGCN)* [139] on spatial-temporal graphs [92, 93]. In their relational reasoning, features of each node were generated with its neighbor nodes in the current frame and consecutive frames by using spatial graph convolution and temporal convolution, respectively. To make inference of the node relation in a more dynamic manner instead of using a constant graph structure, [45] proposed an additional module to adaptively generate conditional edges. Based on the spatio-temporal graph representation, the authors introduced a situational graph generation block that predicted the probability of a link between any two nodes (see Fig. 11d). This block was trained by the mean-square loss over the actual change degree of each link so that the additional connections reflected the categorical information and were closed to the actual facial variations.

Alternatively, the approach of spectral GCN [140] has also been studied. [89] performed the relational reasoning on a spatial-level NPI graph by using graph convolutions in the frequency domain. Each GCN block contained a graph signal filtering layer and a graph coarsening layer. Every two matched nodes were merged into a new node, and the weight of the new node was the sum of the weights of two matched nodes. By repeating this operation several times, one FC layer and one *softmax* layer were added for facial affect classification.

#### 4.3.2 Graph attention network

*Graph Attention Networks (GATs)* aim to strengthen the node connections with high contribution and offer a more flexible way to process the graph structure [141]. [102] introduced an uncertain GNN with GAT as the backbone. The aim is to select the useful edges and depress the noisy edges and learn the AU dependencies on its AU-map graph. In addition, the underlying uncertainties were considered in a probabilistic way, close to the idea of *Bayesian* methods

in GNN [142], to alleviate the data imbalance by weighting the loss function. On the other hand, GAT collaboratively worked with GCN in [66] to deal with two-stream graph inputs. Different from directly applying GAT to achieve the attention, [43] proposed a graph attention convolutional network that added a self-attention graph pooling layer after concatenating three sequential GCN layers (see Fig. 11e). A similar block was done in [115] which revised the GCN block with series attention of channel and node. This improved the reasoning process on graph representations because only important nodes would be aggregated which contained both affective information and facial topology.

#### 4.3.3 Other graph network

According to the structured knowledge organized from an AU-map graph, [29] exploited a *Gated Graph Neural Network* (GGNN) [143] to propagate node information. Similar to RNNs, it calculated the hidden state of the next time-step by jointly considering the current hidden state of each node and its adjacent node. The relational reasoning could be done through the iterative update of GGNN over the graph representation. In [103], a hybrid GNN composed of different dynamic *Multilayer Perceptrons* (MLPs) performed multiple types of message passing, which provided more complementary information for reasoning the positive and negative dependencies among AU nodes.

### 4.4 Traditional Machine Learning Model

Although refining deep features extracted by parameterized neural networks and gradient-based methods is the current mainstream, they require numerous training samples for effective learning. Due to the insufficient data in the early years or the purpose of efficient computation, many non-deep machine learning techniques have been applied for affective graph relational reasoning. Graph structure learning is one of the widely used approaches. In [80], the reasoning of its spatial graph representation was conducted by *LT* learning. Parameters update and graph-edit of *LT* structure were performed iteratively to maximize the marginal log-likelihood of a set of training data. [104] employed *CRF* to infer AU dependencies in an AU-map graph. The use of *copula* functions allowed it to easily model non-linear dependencies among nodes, while an iterative balanced batch learning strategy was introduced to optimize the most representative graph structure by updating each set of parameters with batches. Approaches of graph feature selection are also exploited in this part, including *Correlation-based Feature Selection* (CFS) [74], *Graph Embedding* [72], *Graph Sparse Coding* (GSC) [87] and *Frequent Sub-graphs Mining* [82]. These methods have provided a more diverse concept for graph relational reasoning.

### 4.5 Discussion

Relational reasoning is a significant characteristic of graph-based methods compared to other FAA systems. Although different approaches can be exploited to achieve this purpose, drawbacks of the aforementioned four types are discussed as follows.

*Dynamic Bayesian network*: Nearly half of AU-label graph representations employ *DBNs* as their relational reasoning model. However, the representation quality highly relies

on the available training data that need balanced label distribution in both positive-negative samples and categories. This strong assumption will limit the effectiveness of node dependencies learned by *DBNs*. While the work about correcting and generating labels based on *DBN* [46] has been proposed, the current study has revealed the potential of *GCNs* in processing AU-label graphs. Another problem is that *DBNs* can only be combined with facial features as a relatively independent module, and are hard to integrate into an end-to-end learning framework.

*Classical deep model*: Standard deep models, including *CNNs*, *RNNs* and *AEs*, have been explored to conduct graph relational reasoning before the emergence of *GNNs*. Even if they are suitable for more graph representations than *DBNs*, the required additional adjustments in input format or/and network architecture make the implementation inelegant. For example, the modification of convolutions in [40] resulted in losses of node information, while the *RNNs* let node messages only be passed and updated in a specific sequence that suppressed the graph structure [95]. Besides, applying grid models cannot make full use of the advantage of the graph. They focus more on local features of the input, but the global property represented by the graph is also very important for the analysis of facial affects. Thus, we think the specifically designed networks like *GNNs* will become dominant in this part.

*Graph neural network*: *GNNs* are developing techniques in relational reasoning. Architectures with different focuses have been proposed, but have their shortcomings as well. For instance, *GCNs* cannot handle directed edges well (e.g., AU-level graphs), while *GATs* only use the node links without the consideration of edge attributes (e.g., spatial graphs). Besides, due to the low dimension of the nodes in affective graphs, too deep *GNNs* may be counterproductive. In addition, being an auxiliary block or part of the whole framework will influence the construction of *GNNs*. Therefore, how to manage graph representation and relational reasoning using *GNNs* still needs to be explored.

*Traditional methods*: Traditional machine learning models have taken a place in early studies. In fact, advanced techniques like *DBNs* and *GNNs* are partly inspired by them. Nevertheless, one of the reasons they have been replaced is that these approaches need to be designed separately to cope with different graph representations, similar to hand-crafted feature extraction. Hence, it is difficult to form a general framework. On the other hand, larger amounts of training data and richer computing resources allow deep models to perform more effective and higher-order relational reasoning on affective graphs.

## 5 APPLICATIONS AND PERFORMANCE

According to different description models of facial affects, the FAA can be subdivided into multiple applications. Typical output of FAA systems is the label of a basic facial affect or AUs. Recent researches also extend the goal to predict micro-expression or affective intensity labels or continuous affects. In this section, we compare and discuss the graph-based FAA methods presented in this paper from three main application categories: facial expression recognition, AU detection, and micro-expression recognition. Some special studies outside these three will also be evaluated.

TABLE 1  
An Overview of Facial Affect Databases

Database 'year	Samples			Attributes			Graph-based Properties <sup>3</sup>			Special Contents <sup>4</sup>
	Data Type	Subjects	Number	Eli. & Sou. <sup>1</sup>	Affects <sup>2</sup>	B.B. <sup>1</sup>	LM	AU	Dynamic	
CK(+) '10	Sequences	97(123)	486(593)	P & Lab	6B+N(+C)	●	●	● + I	●	/
MMI '10	Images/Videos	75	740/2900	P & Lab	6B+N	○	○	●	● + D	Head pose
Oulu-CASIA '11		Sequences	80	2880	P & Lab	6B	●	○	○	●
DISFA '13	Sequences	27	130,000	S & Lab	6B+N	●	●	● + I	● + F	/
FER-2013 '13	Images	/	35887	S & Web	6B+N	●	○	○	○	Wild
SFEW 2.0 '15	Images	/	1766	S & Movie	6B+N	●	●	○	○	Wild
AFEW 7.0 '17	Videos	/	1809	S & Movie	6B+N	●	●	○	●	Audio, Wild
BU-3DFE '06	Images	100	2500	P & Lab	6B+N	●	●	○	○	3D, Multi-view, I
BU-4DFE '08	Videos	101	606	P & Lab	6B+N	●	●	● + I	●	3D, Multi-view
BP4D '14	Videos	41	328	S & Lab	6B+E+P	●	●	● + I	● + F	3D, Head pose
SMIC '13	Sequences	16	164	S & Lab	3B <sup>†</sup> +N	●	○	○	●	Micro., NIR
CASME II '14	Sequences	35	247	S & Lab	3B <sup>†</sup> +R+O	●	○	●	● + D	Micro.
SAMM '18	Sequences	32	159	S & Lab	6B+C	●	○	●	● + D	Micro.
CAS(ME) <sup>2</sup> '18	Sequences	22	300+57	S & Lab	3B <sup>†</sup> +O	●	○	●	● + D	Macro. & Micro.
EmotioNet '16	Images	/	950,000	S & Web	6B+17Comp.	●	●	● + I	○	Wild
ExpW '18	Images	/	91,793	S & Web	6B+N	●	○	○	○	Multi-sub., Wild
RAF-DB '19	Images	/	29672	S & Web	6B+N+11Comp.	●	●	○	○	Wild
AffectNet '19	Images	/	420,299	S & Web	6B+N+C+O	●	●	○	○	V&A, Wild
EMOTIC '19	Images	/	23,571	S & Web	6B+N+19Comp.	●	○	○	○	V&A, Multi-sub., Wild

<sup>1</sup> Eli.: elicitation; Sou.: source; P: posed; S: spontaneous; B.B.: bounding boxes; LM: landmarks; • = Yes, ○ = No.

<sup>2</sup> 6B: six basic affects; N: neutral; C: contempt; E: embarrassment; P: pain; O: others; R: repression; 3B<sup>†</sup>: three basic affects (positive, negative, surprise); 3B<sup>‡</sup>: three basic affects (happiness, disgust, surprise); Comp.: compound affects.

<sup>3</sup> I: intensity annotation; D: onset-apex-offset annotation; F: frame-level annotation.

<sup>4</sup> NIR: near-infrared; Multi-sub.: multiple subjects per image; Micro.: micro-expression; Macro.: macro-expression; Wild: in-the-wild; V&A: valence and arousal.

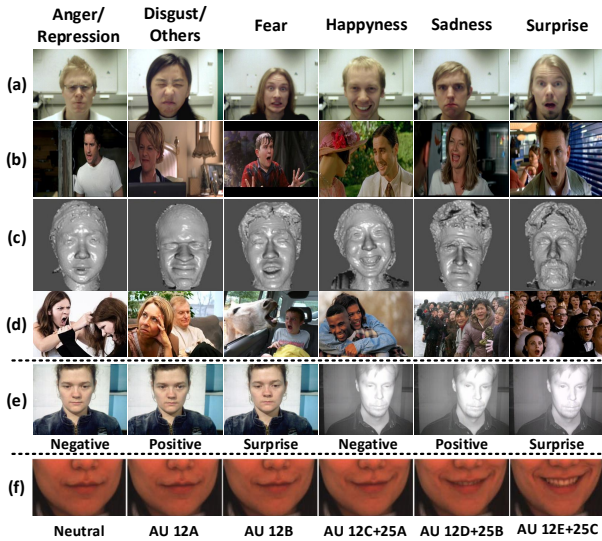


Fig. 12. Facial affect databases. (a) Oulu-CASIA contains posed facial affects; (b) SFEW 2.0 has facial affects under in-the-wild scenarios; (c) BP4D provides 3D affective face images; (d) EMOTIC, multiple faces appear per image with V-A annotations; (e) The SMIC collects images of spontaneous micro facial affects in both visual light and near infrared light; (f) DISFA offers frame-level AU intensity labels.

## 5.1 Databases

Public databases of facial affect are applied as validation material in most FAA studies. A comprehensive overview is presented in Table 1. The characteristics of these databases are listed from four aspects: samples, attributes, graph-related properties and special contents. Figure 12 exhibits several examples of facial affects under different conditions. In addition, for better interpreting the graph-based FAA, we summarize corresponding elements (e.g., landmark coordinates, AU labels) self-carried by databases, which are rarely considered in previous related surveys.

Databases containing posed facial affects, including Ex-

tended Cohn-Kanade Dataset (CK+) [65, 146], M&M Initiative Facial Expression Database (MMI) [147] and Oulu-CASIA NIR&VIS Facial Expression Database (Oulu-CASIA) [148], are chosen by early FAA methods. More challenging databases, such as FER-2013 [149], Static Facial Expression in the Wild (SFEW) 2.0 [150] and Acted Facial Expression in the Wild (AFEW) 7.0 [151], tend to acquire spontaneous affective data from complex and wild environment.

Some databases also contain intensity labels of facial affects and even AUs, e.g., Denver Intensity of Spontaneous Facial Action Database (DISFA) [152], Binghamton University 3D/4D Facial Expression Database (BU-3DFE/4DFE) [153, 154] and Binghamton-Pittsburgh 3D Dynamic Spontaneous Facial Expression Database (BP4D) [155].

Another type of database is for micro-expressions. Participants are required to keep a neutral face while watching videos associated with induction of specific affects [156]. Following this setting, Spontaneous Micro Facial Expression Database (SMIC) [157], Improved Chinese Academy of Sciences Micro-Expression Database (CASME II) [158], Spontaneous Micro-Facial Movement Database (SAMM) [159], Chinese Academy of Sciences Macro-Expression and Micro-Expression Database (CAS(ME)<sup>2</sup>) [160] have been released. However, due to the subtle, rapid, and involuntary nature, it is hard to collect and annotate large-scale micro-expression data with uncontrolled scenarios.

Recently, several large-scale databases have been developed to provide massive data with spontaneous facial affects and in-the-wild conditions, such as Real-World Affective Face Database (RAF-DB) [161], Large-Scale Face Expression in-the-Wild dataset (ExpW) [8], EMOTIC [162], AffectNet [163], EmotioNet [164].

Concerning graph-based FAA, it is available to find and select suitable databases with corresponding metadata, such as landmarks, AU labels, and dynamics, for different graph representation purposes. However, existing databases



TABLE 2  
Performance summary of representative graph-based FER methods discussed in this Paper

References	Prep. <sup>1</sup>		Representation <sup>2</sup>			Reasoning		Posed Database <sup>1</sup>	Wild Database	Validation <sup>3</sup>
	B.B.	LM	Category	Node	Edge	Model	Classifier			
Kotsia and Pitas [85]	○	104	$S : \mathcal{L}$	$\mathbb{C}$	$\Delta$	Tracking	SVM	CK ar: 0.997	/	LO CV
Zafeiriou and Pitas [88]	●	/	$S : \mathcal{R}$	NM	L	Tracking	EGM	CK ar: 0.971	/	LO CV
Tanchotsrinon et al. [73]	●	14	$S : \mathcal{L}$	$\mathbb{C}$	M+E	/	MLP	CK ar: 0.9524	/	HO
Mohseni et al. [81]	○	50	$S : \mathcal{L}$	$\mathbb{C}$	M+E	Tracking	Adaboost	MMI ar: 0.877	/	10F CV
Rivera and Chae [94]	●	/	$ST : \mathcal{R}$	Histograms	DNG	Tracking	SVM	CK+ ar: 1; MMI ar: 0.976; Oulu ar: 0.984	/	10F CV
Yao et al. [69]	●	/	$S : \mathcal{R}$	LBP	L	/	SVM CNN	/	SFEW ar: 0.5538; AFEW ar: 0.5380;	HO
Durmuşoğlu and Kahraman [74]	●	18	$S : \mathcal{L}$	$\mathbb{C}$	F+E	CFS	MLP	MUG [144] ar: 0.9122	/	HO
Dapogny et al. [44]	●	49	$S : \mathcal{L}$	C+HOG	$\Delta$	AE	RF	CK+ ar: 0.934; BU-4DFE ar: 0.750	SFEW ar: 0.371	10F-SI CV HO
Zhong et al. [28]	●	46	$S : \mathcal{L}$	Gabor	F+E	BRNN	SoftMax	CK+ ar: 0.9827; MMI ar: 0.9444; Oulu ar: 0.9306	/	10F-SI CV
Wu et al. [89]	●	/	$S : \mathcal{R}$	Pixel	$\mathbb{E}$	GCN	SoftMax	CK+ ar: 0.9978; JAFEE [145] ar: 0.9444	/	HO
Chen et al. [47]	●	/	$AU : \mathcal{B}$	$\Phi$	KNN	/	SoftMax	CK+ ar: 0.9308; MMI ar: 0.7049; Oulu ar: 0.6385	SFEW ar: 0.5650; RAF ar: 0.8553; AffNet ar: 0.5935	CD
Liu et al. [40]	●	68	$S : \mathcal{L}$	C+HOG	$\Delta$	CNN	SoftMax	CK+ ar: 0.9767; MMI ar: 0.8011	SFEW ar: 0.5536	10F-SI CV HO
Xie et al. [91]	●	/	$S : \mathcal{R}$	ResNet	K-means	GCN	SoftMax	CK+ ar: 0.8527; JAFEE [145] ar: 0.6150	SFEW ar: 0.5643; FER2013 ar: 0.5895 ExpW ar: 68.50%	CD
Zhou et al. [92]	●	34	$ST : \mathcal{L}$	C+HOG	M+H	GCN	SoftMax	CK+ ar: 0.9863; Oulu ar: 0.8723	/	10F-SI CV
Hassan and Mohammed [82]	○	20	$S : \mathcal{L}$	$\mathbb{C}$	F+E	Graph mining	MLP	CK+ ar: 0.9863; Oulu ar: 0.8723	/	HO
Liu et al. [95]	●	/	$ST : \mathcal{F}$	VGG	F	GCN	LSTM	CK+ ar: 0.9954; Oulu ar: 0.9104; MMI ar: 0.8589	/	10F-SI CV
Zhou et al. [45]	●	44	$ST : \mathcal{L}$	C+HOG	L+H	GCN	SoftMax	CK+ ar: 0.9892; Oulu ar: 0.8750	AFEW ar: 0.4512	10F-SI CV HO
Cui et al. [41]	○	/	$AU : \mathcal{B}$	CNN	$\Phi$	DBN	SoftMax	CK+ ar: 0.9759; BP4D ar: 0.8382; MMI ar: 0.8490	EmotioNet ar: 0.9555	5F-SI CV
Liu et al. [115]	●	40	$S : \mathcal{L}$	C+HOG+Gabor /C+CNN	L+H /L+E	GCN	SoftMax	CK+ ar: 0.9923; Oulu ar: 0.9088; MMI ar: 0.8575	SFEW ar: 0.5742 RAF ar: 0.8713	10F-SI CV HO

<sup>1</sup> Prep.: processing; B.B.: bounding boxes; ● = Yes, ○ = No; LM: landmarks; ar: average accuracy rate.

<sup>2</sup>  $S/ST/AU$ : {spatial; spatio-temporal; AU-level} representation;  $: \mathcal{L}/\mathcal{R}/\mathcal{F}$ : {landmark; region; frame}-level graph;  $\mathbb{C}$ : landmark coordinates;  $\Phi$ : label distributions;  $\Delta$ : triangulation; L/M/F: {learning; manual; full} connections;  $\mathbb{E}$ : Euclidean distance;  $\mathbb{H}$ : Hop distance.

<sup>3</sup> CV: cross validation; LO: leave-one-out; HO: holdout validation; 10F: 10-folds; SI: subject independent; CD: cross database validation.

also have some shortcomings. On one hand, no or not accurate enough AU annotations are provided by in-the-wild databases, which limits the role that AUs can play in FAA. On the other hand, there is still a blank in the field of the dynamic large-scale affective database, so that it is hard to use temporal information to generate affective graph representation. Finally, instead of discrete categories, databases about natural and spontaneous facial affects in a continuous domain need more attention.

## 5.2 Facial Expression Recognition

Facial expression recognition (FER), or namely macro-expression recognition, has been working on the topic of basic facial affects classification. A certain trend of FER is that the research focus has shifted from the early posed facial affects in controlled conditions to the recent sponta-

neous facial affects in real scenarios. In other words, the recognition of the former is considered as a solved problem for FAA methods including graph-based FER, which can be corroborated from the results in Table 2. For example, the performance on CK+ database is very close to 100% [85, 89, 94, 95, 115].

From the view of the representation, spatial graphs and spatio-temporal graphs are dominant. The only exception is [47] where the authors utilized the auxiliary label space graphs of the landmark detection and AU detection to approximately learn the label distribution of facial affects. For the two mainly used graph representations, hand-crafted features (e.g., LBP [69], Gabor [28, 115], HOG [40, 92]) or deep-based features (e.g., CNN [115], VGG [95], ResNet [43]) are employed to enhance the node representation similar to many non-graph FER methods [27, 35]. For reasoning

TABLE 3  
Performance summary of representative graph-based AUD methods discussed in this Paper

References	Prep. <sup>1</sup>		Representation <sup>2</sup>			Reasoning		Database <sup>3</sup>	Validation <sup>4</sup>
	B.B.	LM	Category	Node	Edge	Model	Output		
Tong et al. [96]	•	/	$AU : \mathcal{B}$	<i>Gabor</i>	$\Phi$	<i>DBN</i>	<i>Adabst</i>	CK <i>ar</i> : 0.9933; MMI (CK) <i>ar</i> : 0.939	LOSO CV CD
Zhu et al. [97]	•	49	$AU : \mathcal{B}$	C+ <i>Gabor</i>	$\Phi$	<i>DBN</i>	<i>MPE</i>	CK+ <i>ar</i> : 90.48%, $f_1$ : 0.7072; DISFA <i>ar</i> : 93.56%, $f_1$ : 0.7095	2F, 10F CV
Kaltwang et al. [80]	◦	66	$S : \mathcal{L}$	$\mathbb{C}$	$L$	<i>LT</i>		DISFA <i>corr</i> : 0.43, <i>mse</i> : 0.39, <i>icc</i> : 0.36	9F CV
Sechkova et al. [72]	◦	49	$S : \mathcal{L}$	C+ <i>SIFT</i>	$L$	<i>Graph Embedding</i>	<i>SVM</i>	CK+ <i>ar</i> : 0.927	LOSO CV
Walecki et al. [104]	◦	/	$AU : \mathcal{M}$	<i>CNN</i>	$L$	<i>CRF</i>	<i>Ordinal Regression</i>	FERA 2015 [165] <i>icc</i> : 0.63, <i>mae</i> : 1.23; DISFA <i>icc</i> : 0.45, <i>mae</i> : 0.61	HO
Corneanu et al. [100]	•	/	$AU : \mathcal{M}$	<i>VGG</i>	$\Phi$	<i>RNN</i>	<i>Sigmoid</i>	BP4D $f_1$ : 0.617; DISFA $f_1$ : 0.567	3F-SI CV
Dapogny et al. [44]	•	49	$S : \mathcal{L}$	C+HOG	$\Delta$	<i>AE</i>	<i>RF</i>	CK+ <i>auc</i> : 0.953, $f_1$ : 0.788, $nf_1$ : 0.865; BP4D: <i>auc</i> : 0.727, $f_1$ : 0.557, $nf_1$ : 0.636; DISFA <i>auc</i> : 0.824, $f_1$ : 0.491	10F-SI CV
Li et al. [29]	•	20	$AU : \mathcal{M}$	C+ <i>VGG</i>	$M+L$	<i>GGNN</i>	<i>FC</i>	BP4D <i>auc</i> : 0.741, $f_1$ : 0.629; DISFA <i>auc</i> : 0.807, $f_1$ : 0.559	No report
Niu et al. [101]	•	/	$AU : \mathcal{M}$	$\mathbb{W}$	$L$	<i>GCN</i>	<i>FC</i>	BP4D $f_1$ : 0.598; EmotionNet $f_1$ : 0.681	3F-SI CV HO
Liu et al. [86]	•	19	$S : \mathcal{R}$	<i>EAC-Net</i> + <i>AE</i>	$M$	<i>GCN</i>	<i>FC</i>	BP4D <i>auc</i> : 0.873, $f_1$ : 0.628; DISFA <i>auc</i> : 0.746, $f_1$ : 0.550	3F-SI CV
Fan et al. [42]	•	20	$S : \mathcal{R}$	<i>ResNet</i>	KNN+E	<i>DG-CNN</i>	<i>Heatmap Regression</i>	BP4D <i>icc</i> : 0.72, <i>mae</i> : 0.58; DISFA <i>icc</i> : 0.47, <i>mae</i> : 0.20	3F-SI CV
Liu et al. [40]	•	68	$S : \mathcal{L}$	C+HOG	$\Delta$	<i>CNN</i>	<i>FC</i>	CK+ <i>auc</i> : 0.929	10F-SI CV
Zhang et al. [30]	•	18	$S : \mathcal{R}$	<i>HRNetV2</i>	$L$	<i>GCN</i>	<i>Heatmap Regression</i>	BP4D $f_1$ : 0.635; DISFA $f_1$ : 0.620	3F-SI CV
Zhou et al. [105]	•	/	$AU : \mathcal{M}$	<i>Optical-flow</i> + <i>Inception</i>	$L$	<i>GCN</i>	<i>Softmax</i>	CASME II (SAMM) $f_1$ : 0.6110; SAMM (CASME II) $f_1$ : 0.5722	LOSO CV CD
Cui et al. [46]	◦	51	$AU : \mathcal{B}$	<i>LBP</i>	$\Phi$	<i>DBN</i>	<i>LR</i> / <i>CNN</i> / <i>SVM</i>	CK+ $f_1$ : 0.830; BP4D $f_1$ : 0.687; EmotionNet $f_1$ : 0.626; MMI (CK+) $f_1$ : 0.532	5F-SI CV CD
Cui et al. [41]	◦	/	$AU : \mathcal{B}$	<i>VGG</i>	$\Phi$	<i>DBN</i>	<i>FC</i>	CK+ $f_1$ : 0.74; BP4D $f_1$ : 0.57; MMI $f_1$ : 0.58	5F-SI CV
Song et al. [102]	•	/	$AU : \mathcal{M}$	<i>ResNet</i>	<i>Random Mask</i>	<i>GAT</i>	<i>Softmax</i>	BP4D <i>ar</i> : 0.782, $f_1$ : 0.633; DISFA <i>ar</i> : 0.934, $f_1$ : 0.600	3F-SI CV
Song et al. [103]	•	/	$AU : \mathcal{M}$	<i>ResNet</i>	$\Phi$	<i>Hybrid GNN</i>	<i>Softmax</i>	BP4D $f_1$ : 0.634; DISFA $f_1$ : 0.610	3F-SI CV
Song et al. [31]	•	/	$AU : \mathcal{M}$	<i>ResNet</i>	$\Phi$	<i>GCN+LSTM</i>	<i>Softmax</i>	FERA 2015[165] <i>icc</i> : 0.72, <i>mae</i> : 0.57; DISFA <i>icc</i> : 0.56, <i>mae</i> : 0.22	3F-SI CV

<sup>1</sup> Prep.: processing; B.B.: bounding boxes; • = Yes, ◦ = No; LM: landmarks.

<sup>2</sup>  $S/AU$ : {spatial; AU-level} representation;  $\mathcal{L}/\mathcal{R}/\mathcal{B}/\mathcal{M}$ : {landmark; region; label; map}-level graph;  $\mathbb{C}$ : landmark coordinates;  $\Phi$ : label distributions;  $\Delta$ : triangulation;  $L/M$ : {learning; manual} connections;  $\mathbb{E}$ : Euclidean distance.

<sup>3</sup> *ar*: average accuracy rate;  $f_1$ : F1 score;  $nf_1$ : F1-norm score; *corr*: Pearson correlation coefficient; *mae*: mean absolute error; *mse*: mean squared error; *icc*: intra-class correlation coefficient, ICC(3,1); *auc*: area under the receiver operating characteristic curve; DB1 (DB2): train on DB2, test on DB1.

<sup>4</sup> CV: cross validation; LOSO: leave-one-subject-out; (K)F: k-folds; SI: subject independent; HO: holdout validation; CD: cross database validation.

approaches, early studies prefer to capture the relations of an individual node from predefined graph structures using tracking strategies [81, 85, 88, 94] or traditional machine learning models (e.g., *RF* [44], *BRNN* [28], *CNN* [40]). In some of the latest work, *GCNs* become one of the mainstream choice and show state-of-the-art performances on both posed and in-the-wild databases [43, 89, 95, 115]. Another observation is that the framework of combining the spatio-temporal graph representation and *GNNs* is getting more attention in FER studies [45, 92, 95].

Despite many graph-based studies have shown improvements in predicting facial affects, there are still some potential topics for FER. One thing is that the goal of existing methods stays on classifying basic facial affects. No study of using graph-based methods to recognize compound affects (or mixture affects), whose labels are provided by recent databases like RAF-DB and EmotionNet, is reported. One possible solution is to introduce AU-level graph represen-

tations that can describe fine-grained macro-expressions with closer inter-class distances. The other topic is effective graph-based representations due to the big gap between the performance of current methods and the acceptable result in practice when analyzing in-the-wild facial affects. In addition, since existing databases lack sufficient dynamic annotated samples, the evaluation of spatio-temporal graphs in large-scale conditions remains to be explored.

### 5.3 Action Unit Detection

The AU detection (AUD) facilitates a comprehensive analysis of the facial affect and is typically formulated as a multi-task problem that learns a two-class classification model for each AU. It can not only expand the recognition categories of macro-expressions through the AU combination [80], but also can be used as a pre-step to enhance the recognition of micro-expressions [105]. Comparing with graph-based FER, the wide usage of graph structures has a long history in AU detection [38] and has played a more dominant role. Table 3

TABLE 4  
Performance summary of representative graph-based MER methods discussed in this Paper

References	Prep. <sup>1</sup>		Representation <sup>2</sup>			Reasoning		Database <sup>3</sup>	Validation <sup>4</sup>
	B.B.	LM	Category	Node	Edge	Model	Classifier		
Lo et al. [98]	•	/	$AU : \mathcal{B}$	One-hot	$\Phi + KNN$	GCN	Softmax	CASME II (7 cl.) $ar$ : 0.4271	LOSO CV
Lei et al. [70]	•	28	$S : \mathcal{L}$	TCN	$F$	Graph-TCN	Softmax	CASME II (5 cl.) $ar$ : 0.7398, $f_1$ : 0.7246; SAMM (5 cl.) $ar$ : 0.7500, $f_1$ : 0.6985; SAMM (4 cl.) $ar$ : 0.8050, $f_1$ : 0.7657	LOSO CV
Xie et al. [43]	•	/	$AU : \mathcal{M}$	3DCNN	$L$	GCN	Softmax	CASME II (3 cl.) $ar$ : 0.712, $f_1$ : 0.355; CASME II (7 cl.) $ar$ : 0.561, $f_1$ : 0.394; SAMM (3 cl.) $ar$ : 0.702, $f_1$ : 0.433; SAMM (8 cl.) $ar$ : 0.523, $f_1$ : 0.357 SMIC (CASME II) (3 cl.) $ar$ : 0.344, $f_1$ : 0.319; SMIC (SAMM) (3 cl.) $ar$ : 0.451, $f_1$ : 0.309	LOSO CV CD
Buhari et al. [77]	•	68	$S : \mathcal{L}$	$\mathbb{C}$	$F + E + G$	/	SVM	SMIC (3 cl.) $ar$ : 0.7667, $f_1$ : 0.75; CASME II (5 cl.) $ar$ : 0.7504, $f_1$ : 0.74; CAS(II) <sup>2</sup> (4 cl.) $ar$ : 0.8185, $f_1$ : 0.80; SAMM (7 cl.) $ar$ : 87.33%, $f_1$ : 0.87	LOSO CV
Zhou et al. [105]	•	/	$AU : \mathcal{M}$	Optical-flow +Inception	$L$	GCN	Softmax	CASME II (SAMM) $war$ : 0.708, $uar$ : 0.595; SAMM (CASME II) $war$ : 0.662, $uar$ : 0.588; CASME II+SAMM $f_1$ : 0.685, $wf_1$ : 0.742	LOSO CV CD
Liu et al. [87]	•	66	$S : \mathcal{R}$	Optical-flow	$KNN$	GSC	SVM	SMIC (3 cl.) $ar$ : 0.6795, $f_1$ : 0.6844; CASME I [166] (4 cl.) $ar$ : 0.7219, $f_1$ : 0.7236; CASME II (5 cl.) $ar$ : 0.6356, $f_1$ : 0.6364	LOSO CV
Kumar and Bhanu [66]	•	51	$S : \mathcal{L}$	$\mathbb{C} + \text{Optical-flow}$	$M + L$	GCN+GAT	Softmax	CASME II (3 cl.) $ar$ : 0.8966, $f_1$ : 0.8695; CASME II (5 cl.) $ar$ : 0.8130, $f_1$ : 0.7090; SAMM (3 cl.) $ar$ : 0.8872, $f_1$ : 0.8118; SAMM (5 cl.) $ar$ : 0.8824, $f_1$ : 0.8279	LOSO CV
Lei et al. [99]	•	30	$AU : \mathcal{B}$	Embedding	$\Phi$	GCN	Softmax	CASME II (4 cl.) $ar$ : 0.8080, $f_1$ : 0.7871; CASME II (5 cl.) $ar$ : 0.7427, $f_1$ : 0.7047; SAMM (4 cl.) $ar$ : 0.8239, $f_1$ : 0.7735; SAMM (5 cl.) $ar$ : 0.7426, $f_1$ : 0.7045	LOSO CV

<sup>1</sup> Prep.: processing; B.B.: bounding boxes; • = Yes, ○ = No; LM: landmarks.

<sup>2</sup>  $S/AU$ : {spatial; AU-level} representation;  $\mathcal{L}/\mathcal{B}/\mathcal{M}$ : {landmark; label; map}-level graph;  $\mathbb{C}$ : landmark coordinates;  $\Phi$ : label distributions;  $L/F$ : {learning; fully} connections;  $E$ : Euclidean distance;  $G$ : Gradient using slope equation.

<sup>3</sup>  $ar$ : average accuracy rate;  $f_1$ : F1 score;  $war$ : weighted average recall;  $wf_1$ : weighted F1 score;  $uar$ : unweighted average recall; (N) cl.: (N) affective classes; DB1 (DB2): train on DB2, test on DB1.

<sup>4</sup> CV: cross validation; LOSO: leave-one-subject-out; CD: cross database validation.

presents a summary of graph-based AU detection methods including the performance comparison.

Specifically, spatial graphs and AU-level graphs are equally popular in the representation part of AUD. An interesting observation is that, no matter landmark-level or region-level, all the spatial graphs constructed in the listed AUD methods employed facial landmarks [30, 40, 42, 44, 72, 80, 86]. The possible reason is that the landmark information is helpful and effective for locating the facial areas where AUs may occur. In this setting, their node representations are close to that in spatial graphs of FER methods, which usually combine geometric coordinates with appearance features (e.g., *SIFT* [72], *HOG* [40, 44]). Although some AUD methods using AU-level graphs also exploited traditional features (e.g., *Gabor* [96, 97], *LBP* [46]) or deep features (e.g., *VGG* [100]) to introduce appearance information, their graph representations were basically initialized from the AU label distribution of the training set. This has made the *DBN* model popular in the relational reasoning stage [46, 96, 97]. Another similar trend to graph-based FER is that *GNNs* have been widely utilized to learn the latent dependency among individual AUs in recent studies, such as *GCN* [30, 86, 101, 105], *GAT* [102], *GGNN* [29] and *DG-CNN* [42]. But the difference is that *FC* layers [29, 40, 86, 101] or regression models [30, 42, 104] are often applied for predicting labels instead of *Softmax* classifier [102, 105].

A special line of AUD research analyzes the facial affects by estimating the AU intensities, which could have greater

information value in understanding complex affective states [167]. Even though a few attempts in estimating AU intensities based on graph structures have existed [42, 80, 100], the study of using the latest spatio-temporal graph representations and *GNNs* has not been reported. Another big challenge in AUD is insufficient and imbalanced samples. The recent graph-based methods using transfer learning [46, 101] or uncertainty learning [102] were proposed to address this problem. They showed an advantage of graph-based method in this topic and are helpful to implement AUD in large-scale unlabeled data.

## 5.4 Micro-Expression Recognition

Micro-expressions are fleeting and involuntary facial affects that people usually exhibit in high stake situations when attempting to conceal or mask their true feelings [156]. The earliest well-known studies came from [173] as well as [174]. Generally, a micro-expression only lasts from 1/25 to 1/2 seconds long and is too subtle and fleeting for an untrained person to perceive. Therefore, developing an automatic micro-expression recognition (MER) system is valuable in reading human hidden affective states. Besides the short duration, the characteristics of low intensity and localization also make it challenging.

To this end, graph-based MER methods have been designed to address the above challenges, and have become appealing in the past two years [87], especially in 2020 [43, 70, 77, 98, 105]. Table 4 lists the reported performance



TABLE 5  
Performance summary of graph-based methods for special FAA tasks discussed in this Paper

References	Prep. <sup>1</sup>		Representation <sup>2</sup>			Reasoning		Database <sup>3</sup>	Validation <sup>4</sup>
	B.B.	LM	Category	Node	Edge	Model	Output		
Kaltwang et al. [80]	○	66	$S : \mathcal{L}$	$\mathbb{C}$	$L$	$LT$		ShoulderPain [168] <i>corr</i> : 0.23, <i>mse</i> : 0.60	8F CV
Dapogny et al. [44]	●	49	$S : \mathcal{L}$	$\mathbb{C}+HOG$	$\Delta$	$AE$	$RF$	CK+ (eyes occluded) <i>ar</i> : 0.879; CK+ (mouth occluded) <i>ar</i> : 0.727	10F-SI CV
Zhang et al. [90]	●	/	$S : \mathcal{R}$	$VGG$	$L$	$GCN$	$Softmax/FC$	EMOTIC (26 cl.) <i>prc</i> : 0.2842; EMOTIC (VAD) <i>er</i> : 0.9	HO
Chen et al. [93]	●	68	$ST : \mathcal{L}$	$\mathbb{C}$	$\Delta+M$	$GCN$	$FC$	CES [15] <i>val_ccc</i> : 0.515, <i>aro_ccc</i> : 0.513	HO
Zhou et al. [45]	●	44	$ST : \mathcal{L}$	$\mathbb{C}+HOG$	$L+H$	$GCN$	$SoftMax$	CK+ (random occlusion) <i>ar</i> : 0.9551; Oulu (random occlusion) <i>ar</i> : 0.8121 AFEW (random occlusion) <i>ar</i> : 0.4047	10F-SI CV HO
Chien et al. [106]	○	/	$\mathcal{O}$	$3DCNN$	$Transfer Knowledge$	$GCN$	$FC$	Amigos [169] (Ascertain) <i>val_uar</i> : 0.798, <i>aro_uar</i> : 0.679; Ascertain [170] (Amigos) <i>val_uar</i> : 0.704, <i>aro_uar</i> : 0.569	CD
Xu et al. [107]	○	/	$\mathcal{O}$	$AE$	$\Phi$	$GCN$	$GAN$	NVIE [171] <i>ar</i> : 0.5632, $f_1$ : 0.6573, $mif_1$ : 0.6614, $maf_1$ : 0.6412; FilmStim [172] <i>ar</i> : 0.4669, $f_1$ : 0.5782, $mif_1$ : 0.6131, $maf_1$ : 0.5931	HO

<sup>1</sup> Prep.: processing; B.B.: bounding boxes; ● = Yes, ○ = No; LM: landmarks.

<sup>2</sup>  $S/ST/O$ : {spatial; spatio-temporal; other} representation;  $\mathcal{L}/\mathcal{R}$ : {landmark; region}-level graph;  $\mathbb{C}$ : landmark coordinates;  $\Phi$ : label distributions;  $\Delta$ : triangulation;  $M/L$ : {manual/learning} connections;  $Trans. K$ : transfer knowledge.

<sup>3</sup> *corr*: Pearson correlation coefficient; *mes*: mean squared error; *prc*: area under the precision recall curves; *er*: average error rate; *val/aro*: valance/arousal; *ccc*: concordance correlation coefficient; *uar*: unweighted average recall; (N) cl.: (N) affective classes; VAD: valence, arousal, dominance; DB1 (DB2): train on DB2, test on DB1; *ar*: average accuracy rate;  $f_1$ : F1 score;  $mif_1$ : micro F1 score;  $maf_1$ : macro F1 score.

<sup>4</sup> CV: cross validation; (K)F: k-folds; SI: subject independent; HO: holdout validation; CD: cross database validation.

of a few representative recent studies of graph-based MER. In terms of representation types, these methods fall into the landmark-level spatial graph [70, 77, 87] and the AU-level graph [43, 98, 105]. For the former, their idea is to use landmarks to locate and analyze specific facial areas to deal with the local response and the subtleness of micro-expressions. For the latter, they aim to infer the AU relationship to improve the final performance. The difference in processing ideas is also reflected in the reasoning procedure. Approaches like GSC [87] and variant CNN [70] are exploited in the landmark-level graph to integrate the individual node feature representations. While the GCN is employed to learn an optimal graph structure of the AU dependency knowledge from training data and make predictions. But one common thing is that almost all the methods except [77] consider the local appearance in a spatio-temporal way by using *optical-flow* or *DNNs*.

A problem in graph-based MER is the lack of large-scale in-the-wild data. The small sample size limits the AU-level graph representation that relies on initializing the AU relationship from the AU label distribution of the training set. The lab-controlled data make it difficult to follow the trend in FER studies, which generalizes the graph-based FAA methods in real-world scenarios. However, the analysis of uncontrolled micro-expressions is very important, because micro-expressions and macro-expressions can occur simultaneously in many real cases. For example, furrowing on the forehead slightly and quickly when smiling indicates the true feeling of a person [174]. For another thing, since the evolutionary appearance information is crucial for the micro-expression analysis, building a spatio-temporal graph representation that can model the duration and the dynamic of micro-expressions is also a helpful but unexplored topic.

## 5.5 Special Tasks

The graph-based methods also play an important role in several special FAA tasks, such as pain detection [80], non-basic affect recognition [90], occluded FER [44, 45], multi-modal affect recognition [93, 106] and affect tagging [107].

Table 5 lists a summary of the latest graph-based FAA methods for special tasks. For graph constructions including two special representations [106, 107], the strategies of their node representations and edge initialization are similar to that in graph-based FER, MER, and AUD methods. While for the reasoning step, GCN is the top-1 option. This observation implies that the framework of the graph-based method discussed in this paper can be easily extended to many other FAA tasks and promote performance improvement.

## 6 CONCLUSION

In this article, a comprehensive review has been given into the appealing field of the graph-based FAA. Finally, we provide an overall discussion and highlight open directions in this section.

### 6.1 Discussion

The graph-based FAA methods have been dissected into fundamental components for elaboration and discussion of their potential and limitations. We have started by introducing background and pre-steps. An in-depth discussion about two major aspects has been followed, including the different kinds of graph-based affective representations and their corresponding relational reasoning models. The performance of representative studies on public databases has been summarized in terms of facial expression recognition, micro-expression recognition, action unit detection, and other special FAA applications.

#### 6.1.1 Representation

When encoding facial affect into graph representations, strategies vary according to node elements and edge elements. Specifically, the spatial graph regards an affective face as multiple local crucial facial areas and model the relationship among them, while the spatio-temporal graph also considers the temporal evolution in continuous frames. Another distinctive representation is the AU-level graph. Since each AU and its co-occurrence dependency provide certain semantics of facial affects, most of the AU-level graphs are built by learning a distribution from existing available data.

Other representations like multi-modal graphs employ the graph structure as a bridge to establish the information interaction from different modalities.

There are various techniques for generating node attributes and initializing edge connections. The appearance and geometric information can be separately or jointly extracted by either pre-defined descriptors or deep models for each node, while the edge links can be obtained through manual linking, automatic learning, or calculation rules. Regardless of these approaches, the node attribute generation and the edge connection initialization are followed by most methods. Therefore, spatial graphs and AU-level graphs are slightly different depending on the node element, but they can share the similar node attributes (e.g., landmark coordinates [29, 40]) or edge connections (e.g., KNN [42, 47]). For the temporal domain, some methods also exploited the dynamic information in the representation stage [43, 87, 105], even though they did not construct a whole space-time representation like spatio-temporal graphs.

### 6.1.2 Relational reasoning

Relational reasoning approaches infer latent relationships or inherent dependencies of graph nodes in terms of space, time, semantic, etc. The category of front graph representation will affect the technique choice of relational reasoning to a certain extent. Both traditional and advanced machine learning methods have been proposed to conduct relational reasoning on affective graphs. DBNs explicitly update the relevant graph structure along with other pre-extracted local features and have been mostly used for AU-label representations. For deep learning methods, standard models can execute the transformation of input format or adjustment of network architecture to meet the requirements of processing graph relational reasoning, while GNNs deal with structured graph data based on their specially designed architecture. The two types of deep models can contribute to FAA either independently or cooperatively and are versatile for a variety of graph representations. Other basic machine learning methods, including graph structure learning and graph feature selection, have also been provided for relational reasoning. They have become less popular due to applicability and performance limitations.

## 6.2 Open Directions

Despite significant advances, the graph-based FAA is still an appealing field that has many open directions. Due to advantages in modeling and reasoning latent relationships of facial affects, graph-based methods may provide complementary information to help solve some challenges commonly faced by non-graph-based approaches. In other topics, the graph-based method either has natural advantages or unexplored research potential.

### 6.2.1 In-the-wild scenarios

Although many efforts have been done for graph-based FAA in naturalistic conditions [40, 43, 44, 45, 46, 47, 69, 101], even the state-of-the-art performance is far from actual applications. Factors like illumination, head pose, and part occlusion are challenging in constructing an effective graph representation. For one thing, large illumination changes and head pose variations will impair the accuracy of face detection and registration, which is vital for establishing

landmark-level graphs. The graph representation without landmarks [69, 91] should be a possible direction to avoid this problem. For another thing, missing face parts resulted from camera view or context occlusion make it difficult to encode enough facial information and obtain meaningful connections in an affective graph. Pilot work [44, 45] has tried to exploit a sub-graph without masked facial parts or generate adaptive edge links to alleviate the influence. Unfortunately, there still has been a big performance decrease compared to that in normal conditions. Therefore, more effective graph-based representations should be proposed to account for these problems.

### 6.2.2 3D and 4D facial affects

Using 3D and 4D face images might be another reasonable topic because the 3D face shape provides additional depth information and contains subtle facial deformations in a dynamic way so that they are intuitively insensitive to pose and light changes. Some studies have transformed 3D faces to 2D images and generated graph representations [29, 42, 44, 100], but they have not fully taken the advantage of the 3D data. Alternatively, attempts of both non-graph-based [175] and graph-based methods [84] have been explored to directly conduct FAA on 3D or 4D faces. Since the structure of the 3D face mesh is naturally close to the graph structure, employing the graph representation and reasoning to handle 3D face images will promote the improvement of in-the-wild FAA. Besides, there is also a potential topic of using 3D and 4D data with graph-based methods in micro-expression recognition.

### 6.2.3 Valence and arousal

Estimating the continuous dimension is a rising topic in FAA. Not like discrete labels, the valence indicates the positive or negative characteristic of a facial affect, while the arousal denotes the intensity level of the activation about a facial affect. In recent years, some related competitions have been held at CVPR 2017 [12], BMVC 2019 [176] and FG 2020 [177]. Large-scale FAA databases (Aff-Wild I [12], II [177]) containing V-A annotations have been released to support the continuous analysis of facial affects. Several graph-based methods have been proposed to perform the V-A measurement [42, 80, 104] on lab-controlled databases. Although methods like [90] have reported V-A performance on in-the-wild databases, more comprehensive studies should be done to reveal the effectiveness of graph-based methods in analyzing continuous facial affects.

### 6.2.4 Context and multi-modality

Most current FAA methods only consider a single face in one image or one sequence. But in real cases, people usually have affective behaviors including facial expression, body gesture, and emotional speaking [178]. These facial affective displays are highly associated with context surroundings that include but not limit to the affective behavior of other people in social interactions or inanimate objects. Existing studies like [90] and [91] have employed graph reasoning to infer relationships between the target face and other objects in the same image. The facial affects and other helpful contexts can be combined in a graph representation to perform the analysis on a fuller scope. Another reasonable topic is to introduce additional data channels that are

multi-modality. The graph-based methods have also been successfully extended to process multi-modal affect analysis tasks with information such as audio [93] and physiological signal [106], which shows a good research prospect.

### 6.2.5 Cross-database and transfer learning

Insufficient annotations and imbalanced labels are two problems that limit the development of FAA research. One possible solution is to use graph-based transfer learning. Efforts like [46, 101, 102] have exploited the graph structure to solve this challenge in terms of semi-supervision, label correction and generation, or uncertainty measurement. On the other hand, the performance of affective features extracted by using graph-based representation and reasoning has been proved through cross-database validation in all FER [47, 91], MER [43, 105] and AUD [46, 96, 105]. This reveals that the graph-based method is valuable in improving the generalization capability of affective features.

## ACKNOWLEDGMENTS

**Funding:** This work was supported by the China Scholarship Council [CSC, No.202006150091].

The authors would like to thank Muzammil Behzad and Tuomas Varanka for providing materials and suggestions for the Figures used in this paper.

## REFERENCES

- [1] C. Darwin and P. Prodger, *The expression of the emotions in man and animals*. Oxford University Press, USA, 1998.
- [2] M. S. Gazzaniga, R. B. Ivry, and G. Mangun, *Cognitive Neuroscience. The Biology of the Mind*, (2014). Norton: New York, 2014.
- [3] R. W. Picard, E. Vyzas, and J. Healey, "Toward machine emotional intelligence: Analysis of affective physiological state," *IEEE Transactions on Pattern Analysis and Machine Intelligence*, vol. 23, no. 10, pp. 1175–1191, 2001.
- [4] R. E. Jack, O. G. Garrod, H. Yu, R. Caldara, and P. G. Schyns, "Facial expressions of emotion are not culturally universal," *National Academy of Sciences*, vol. 109, no. 19, pp. 7241–7244, 2012.
- [5] E. Sariyanidi, H. Gunes, and A. Cavallaro, "Automatic analysis of facial affect: A survey of registration, representation, and recognition," *IEEE Transactions on Pattern Analysis and Machine Intelligence*, vol. 37, no. 6, pp. 1113–1133, 2014.
- [6] M. G. Calvo, A. Gutiérrez-García, and M. Del Libano, "What makes a smiling face look happy? visual saliency, distinctiveness, and affect," *Psychological Research*, vol. 82, no. 2, pp. 296–309, 2018.
- [7] M. Tavakolian and A. Hadid, "A spatiotemporal convolutional neural network for automatic pain intensity estimation from facial dynamics," *International Journal of Computer Vision*, vol. 127, no. 10, pp. 1413–1425, 2019.
- [8] Z. Zhang, P. Luo, C. C. Loy, and X. Tang, "From facial expression recognition to interpersonal relation prediction," *International Journal of Computer Vision*, vol. 126, no. 5, pp. 550–569, 2018.
- [9] L. Zhao, X. Peng, Y. Tian, M. Kapadia, and D. N. Metaxas, "Towards image-to-video translation: A structure-aware approach via multi-stage generative adversarial networks," *International Journal of Computer Vision*, vol. 128, no. 10, pp. 2514–2533, 2020.
- [10] M. F. Valstar, E. Sánchez-Lozano, J. F. Cohn, L. A. Jeni, J. M. Girard, Z. Zhang, L. Yin, and M. Pantic, "Fera 2017-addressing head pose in the third facial expression recognition and analysis challenge," in *IEEE International Conference on Automatic Face & Gesture Recognition (FG)*. IEEE, 2017, pp. 839–847.
- [11] A. Dhall, G. Sharma, R. Goecke, and T. Gedeon, "EmotiW 2020: Driver gaze, group emotion, student engagement and physiological signal based challenges," in *International Conference on Multimodal Interaction (ICMI)*, 2020, pp. 784–789.
- [12] S. Zafeiriou, D. Kollias, M. A. Nicolaou, A. Papaioannou, G. Zhao, and I. Kotsia, "Aff-wild: valence and arousal in-the-wild challenge," in *IEEE Conference on Computer Vision and Pattern Recognition Workshops (CVPRW)*, 2017, pp. 34–41.
- [13] D. Kollias, I. Kotsia, E. Hajiyeve, and S. Zafeiriou, "Analysing affective behavior in the second abaw2 competition," *arXiv preprint arXiv:2106.15318*, 2021.
- [14] C. F. Benitez-Quiroz, R. Srinivasan, Q. Feng, Y. Wang, and A. M. Martinez, "Emotionet challenge: Recognition of facial expressions of emotion in the wild," *arXiv preprint arXiv:1703.01210*, 2017.
- [15] F. Ringeval, B. Schuller, M. Valstar, N. Cummins, R. Cowie, L. Tavabi, M. Schmitt, S. Alisamir, S. Amiriparian, E.-M. Messner et al., "Avec 2019 workshop and challenge: state-of-mind, detecting depression with ai, and cross-cultural affect recognition," in *International on Audio/Visual Emotion Challenge and Workshop*, 2019, pp. 3–12.
- [16] L. Stappen, A. Baird, G. Rizo, P. Tzirakis, X. Du, F. Hafner, L. Schumann, A. Mallol-Ragolta, B. W. Schuller, I. Lefter et al., "Muse 2020 challenge and workshop: Multimodal sentiment analysis, emotion-target engagement and trustworthiness detection in real-life media: Emotional car reviews in-the-wild," in *International on Multimodal Sentiment Analysis in Real-life Media Challenge and Workshop*, 2020, pp. 35–44.
- [17] P. Ekman and W. V. Friesen, "Constants across cultures in the face and emotion," *Journal of Personality and Social Psychology*, vol. 17, no. 2, pp. 124–129, 1971.
- [18] P. Ekman, "Strong evidence for universals in facial expressions: a reply to russell's mistaken critique," *Psychological Bulletin*, vol. 115, no. 2, pp. 268–287, 1994.
- [19] E. Friesen and P. Ekman, "Facial action coding system: a technique for the measurement of facial movement," *Palo Alto*, vol. 3, no. 2, p. 5, 1978.
- [20] P. Ekman, "Facial action coding system (facs)," *A Human Face*, 2002.
- [21] R. Plutchik, "A general psychoevolutionary theory of emotion," in *Theories of Emotion*. Elsevier, 1980, pp. 3–33.
- [22] M. K. Greenwald, E. W. Cook, and P. J. Lang, "Affective judgment and psychophysiological response: dimensional covariation in the evaluation of pictorial stimuli," *Journal of Psychophysiology*, vol. 3, no. 1, pp. 51–64, 1989.
- [23] J. A. Russell, "Evidence of convergent validity on the dimensions of affect," *Journal of Personality and Social Psychology*, vol. 36, no. 10, p. 1152, 1978.
- [24] V. Sethu, E. M. Provost, J. Epps, C. Busso, N. Cummins, and S. Narayanan, "The ambiguous world of emotion representation," *arXiv preprint arXiv:1909.00360*, 2019.
- [25] D. Kollias, P. Tzirakis, M. A. Nicolaou, A. Papaioannou, G. Zhao, B. Schuller, I. Kotsia, and S. Zafeiriou, "Deep affect prediction in-the-wild: Aff-wild database and challenge, deep architectures, and beyond," *International Journal of Computer Vision*, vol. 127, no. 6, pp. 907–929, 2019.
- [26] L. Yin, X. Chen, Y. Sun, T. Worm, and M. Reale, "A high-resolution 3d dynamic facial expression database," in *IEEE International Conference on Automatic Face and Gesture Recognition (FG)*, 2008, pp. 1–6.
- [27] G. Zhao and M. Pietikainen, "Dynamic texture recognition using local binary patterns with an application to facial expressions," *IEEE Transactions on Pattern Analysis and Machine Intelligence*, vol. 29, no. 6, pp. 915–928, 2007.
- [28] L. Zhong, C. Bai, J. Li, T. Chen, S. Li, and Y. Liu, "A graph-structured representation with brnn for static-based facial expression recognition," in *IEEE International Conference on Automatic Face and Gesture Recognition (FG)*. IEEE, 2019, pp. 1–5.
- [29] G. Li, X. Zhu, Y. Zeng, Q. Wang, and L. Lin, "Semantic relationships guided representation learning for facial action unit recognition," in *AAAI Conference on Artificial Intelligence (AAAI)*, vol. 33, no. 01, 2019, pp. 8594–8601.
- [30] Z. Zhang, T. Wang, and L. Yin, "Region of interest based graph convolution: A heatmap regression approach for action unit detection," in *ACM International Conference on Multimedia (ACM MM)*, 2020, pp. 2890–2898.
- [31] T. Song, Z. Cui, Y. Wang, W. Zheng, and Q. Ji, "Dynamic probabilistic graph convolution for facial action unit intensity estimation," in *Proceedings of the IEEE/CVF Conference on Computer Vision and Pattern Recognition (CVPR)*, 2021, pp. 4845–4854.
- [32] J. F. Cohn and F. De la Torre, *Automated face analysis for affective computing*. Oxford University Press, 2015.
- [33] U. Zarinis and S. Kondrats, *Anatomy for sculptors: understanding the human figure*. Anatomy Next, Incorporated, 2015.
- [34] D. L. Bimler and G. V. Paramei, "Facial-expression affective attributes and their configurational correlates: components and categories," *Spanish Journal of Psychology*, vol. 9, no. 1, p. 19, 2006.
- [35] K. Zhang, Y. Huang, Y. Du, and L. Wang, "Facial expression recognition based on deep evolutionary spatial-temporal networks," *IEEE Transactions on Image Processing*, vol. 26, no. 9, pp. 4193–4203, 2017.
- [36] Y. Li, G. Lu, J. Li, Z. Zhang, and D. Zhang, "Facial expression recognition in the wild using multi-level features and attention mechanisms," *IEEE Transactions on Affective Computing*, 2020.
- [37] G. M. Jacob and B. Stenger, "Facial action unit detection with transformers," in *Proceedings of the IEEE/CVF Conference on Computer Vision and Pattern Recognition (CVPR)*, 2021, pp. 7680–7689.
- [38] B. Martinez, M. F. Valstar, B. Jiang, and M. Pantic, "Automatic analysis of facial actions: A survey," *IEEE Transactions on Affective Computing*, vol. 10, no. 3, pp. 325–347, 2017.
- [39] L. F. Barrett, *How emotions are made: The secret life of the brain*. Houghton Mifflin Harcourt, 2017.
- [40] Y. Liu, X. Zhang, Y. Lin, and H. Wang, "Facial expression recognition via deep action units graph network based on psychological mechanism," *IEEE Transactions on Cognitive and Developmental Systems*, vol. 12, no. 2, pp. 311–322, 2019.
- [41] Z. Cui, T. Song, Y. Wang, and Q. Ji, "Knowledge augmented deep neural networks for joint facial expression and action unit recognition," *Advances in Neural Information Processing Systems*, vol. 33, 2020.
- [42] Y. Fan, J. Lam, and V. Li, "Facial action unit intensity estimation via semantic correspondence learning with dynamic graph convolution," in *AAAI Conference on Artificial Intelligence (AAAI)*, vol. 34, no. 07, 2020, pp. 12701–12708.
- [43] H.-X. Xie, L. Lo, H.-H. Shuai, and W.-H. Cheng, "Au-assisted graph attention convolutional network for micro-expression recognition," in *ACM*



- International Conference on Multimedia (ACM MM)*, 2020, pp. 2871–2880.
- [44] A. Dapogny, K. Bailly, and S. Dubuisson, “Confidence-weighted local expression predictions for occlusion handling in expression recognition and action unit detection,” *International Journal of Computer Vision*, vol. 126, no. 2, pp. 255–271, 2018.
  - [45] J. Zhou, X. Zhang, and Y. Liu, “Learning the connectivity: Situational graph convolution network for facial expression recognition,” in *IEEE International Conference on Visual Communications and Image Processing*. IEEE, 2020, pp. 230–234.
  - [46] Z. Cui, Y. Zhang, and Q. Ji, “Label error correction and generation through label relationships,” in *AAAI Conference on Artificial Intelligence (AAAI)*, vol. 34, no. 04, 2020, pp. 3693–3700.
  - [47] S. Chen, J. Wang, Y. Chen, Z. Shi, X. Geng, and Y. Rui, “Label distribution learning on auxiliary label space graphs for facial expression recognition,” in *IEEE Conference on Computer Vision and Pattern Recognition (CVPR)*, 2020, pp. 13984–13993.
  - [48] C. A. Corneanu, M. O. Simón, J. F. Cohn, and S. E. Guerrero, “Survey on rgb, 3d, thermal, and multimodal approaches for facial expression recognition: History, trends, and affect-related applications,” *IEEE Transactions on Pattern Analysis and Machine Intelligence*, vol. 38, no. 8, pp. 1548–1568, 2016.
  - [49] S. Li and W. Deng, “Deep facial expression recognition: A survey,” *IEEE Transactions on Computing*, 2020.
  - [50] K. M. Goh, C. H. Ng, L. L. Lim, and U. U. Sheikh, “Micro-expression recognition: an updated review of current trends, challenges and solutions,” *The Visual Computer*, vol. 36, no. 3, pp. 445–468, 2020.
  - [51] L. Zhang, B. Verma, D. Tjondronegoro, and V. Chandran, “Facial expression analysis under partial occlusion: A survey,” *ACM Computing Surveys*, vol. 51, no. 2, pp. 1–49, 2018.
  - [52] P. V. Rouast, M. Adam, and R. Chiong, “Deep learning for human affect recognition: Insights and new developments,” *IEEE Transactions on Affective Computing*, 2019.
  - [53] X. Ben, Y. Ren, J. Zhang, S.-J. Wang, K. Kpalma, W. Meng, and Y.-J. Liu, “Video-based facial micro-expression analysis: A survey of datasets, features and algorithms,” *IEEE Transactions on Pattern Analysis and Machine Intelligence*, 2021.
  - [54] A. Mollahosseini, D. Chan, and M. H. Mahoor, “Going deeper in facial expression recognition using deep neural networks,” in *IEEE Winter Conference on Applications of Computer Vision (WACV)*. IEEE, 2016, pp. 1–10.
  - [55] P. Khorrami, T. Le Paine, K. Brady, C. Dagli, and T. S. Huang, “How deep neural networks can improve emotion recognition on video data,” in *IEEE International Conference on Image Processing (ICIP)*. IEEE, 2016, pp. 619–623.
  - [56] P. Viola and M. Jones, “Rapid object detection using a boosted cascade of simple features,” in *IEEE Conference on Computer Vision and Pattern Recognition (CVPR)*, vol. 1. IEEE, 2001, pp. 1–I.
  - [57] X. Zhu and D. Ramanan, “Face detection, pose estimation, and landmark localization in the wild,” in *IEEE Conference on Computer Vision and Pattern Recognition (CVPR)*. IEEE, 2012, pp. 2879–2886.
  - [58] T. F. Cootes, G. J. Edwards, and C. J. Taylor, “Active appearance models,” *IEEE Transactions on Pattern Analysis and Machine Intelligence*, vol. 23, no. 6, pp. 681–685, 2001.
  - [59] K. Zhang, Z. Zhang, Z. Li, and Y. Qiao, “Joint face detection and alignment using multitask cascaded convolutional networks,” *IEEE Signal Processing Letters*, vol. 23, no. 10, pp. 1499–1503, 2016.
  - [60] R. Ranjan, V. M. Patel, and R. Chellappa, “Hyperface: A deep multi-task learning framework for face detection, landmark localization, pose estimation, and gender recognition,” *IEEE Transactions on Pattern Analysis and Machine Intelligence*, vol. 41, no. 1, pp. 121–135, 2017.
  - [61] X. Dong, Y. Yang, S.-E. Wei, X. Weng, Y. Sheikh, and S.-I. Yu, “Supervision by registration and triangulation for landmark detection,” *IEEE Transactions on Pattern Analysis and Machine Intelligence*, 2020.
  - [62] A. Bulat and G. Tzimiropoulos, “How far are we from solving the 2d and 3d face alignment problem?(and a dataset of 230,000 3d facial landmarks),” in *IEEE International Conference on Computer Vision (ICCV)*, 2017, pp. 1021–1030.
  - [63] I. Masi, Y. Wu, T. Hassner, and P. Natarajan, “Deep face recognition: A survey,” in *SIBGRAPI Conference on Graphics, Patterns and Images (SIBGRAPI)*. IEEE, 2018, pp. 471–478.
  - [64] N. Wang, X. Gao, D. Tao, H. Yang, and X. Li, “Facial feature point detection: A comprehensive survey,” *Neurocomputing*, vol. 275, pp. 50–65, 2018.
  - [65] P. Lucey, J. F. Cohn, T. Kanade, J. Saragih, Z. Ambadar, and I. Matthews, “The extended cohn-kanade dataset (ck+): A complete dataset for action unit and emotion-specified expression,” in *IEEE Conference on Computer Vision and Pattern Recognition-Workshops*. IEEE, 2010, pp. 94–101.
  - [66] A. J. R. Kumar and B. Bhanu, “Micro-expression classification based on landmark relations with graph attention convolutional network,” in *Proceedings of the IEEE/CVF Conference on Computer Vision and Pattern Recognition (CVPR)*, 2021, pp. 1511–1520.
  - [67] K. Zhao, W.-S. Chu, and H. Zhang, “Deep region and multi-label learning for facial action unit detection,” in *IEEE Conference on Computer Vision and Pattern Recognition (CVPR)*, 2016, pp. 3391–3399.
  - [68] Y.-H. Oh, J. See, A. C. Le Ngo, R. C.-W. Phan, and V. M. Baskaran, “A survey of automatic facial micro-expression analysis: databases, methods, and challenges,” *Frontiers in Psychology*, vol. 9, p. 1128, 2018.
  - [69] A. Yao, J. Shao, N. Ma, and Y. Chen, “Capturing au-aware facial features and their latent relations for emotion recognition in the wild,” in *ACM on International Conference on Multimodal Interaction (ICMI)*, 2015, pp. 451–458.
  - [70] L. Lei, J. Li, T. Chen, and S. Li, “A novel graph-tcn with a graph structured representation for micro-expression recognition,” in *ACM International Conference on Multimedia (ACM MM)*, 2020, pp. 2237–2245.
  - [71] P. Kakumanu and N. Bourbakis, “A local-global graph approach for facial expression recognition,” in *IEEE International Conference on Tools with Artificial Intelligence (ICTAI)*. IEEE, 2006, pp. 685–692.
  - [72] T. Sechkova, K. Tonchev, and A. Manolova, “Action unit recognition in still images using graph-based feature selection,” in *IEEE 8th International Conference on Intelligent Systems (IS)*. IEEE, 2016, pp. 646–650.
  - [73] C. Tanchotsrinon, S. Phimoltaree, and S. Maneeroj, “Facial expression recognition using graph-based features and artificial neural networks,” in *IEEE International Conference on Imaging Systems and Techniques*. IEEE, 2011, pp. 331–334.
  - [74] A. Durmuşoğlu and Y. Kahraman, “Facial expression recognition using geometric features,” in *International Conference on Systems, Signals and Image Processing*. IEEE, 2016, pp. 1–5.
  - [75] M. Sabzevari, S. Toosizadeh, S. R. Quchani, and V. Abrishami, “A fast and accurate facial expression synthesis system for color face images using face graph and deep belief network,” in *International Conference on Electronics and Information Engineering*, vol. 2. IEEE, 2010, pp. V2–354.
  - [76] V. Kazemi and J. Sullivan, “One millisecond face alignment with an ensemble of regression trees,” in *IEEE Conference on Computer Vision and Pattern Recognition (CVPR)*, 2014, pp. 1867–1874.
  - [77] A. M. Buhari, C.-P. Ooi, V. M. Baskaran, R. C. Phan, K. Wong, and W.-H. Tan, “Facs-based graph features for real-time micro-expression recognition,” *Journal of Imaging*, vol. 6, no. 12, p. 130, 2020.
  - [78] N. Dalal and B. Triggs, “Histograms of oriented gradients for human detection,” in *IEEE Conference on Computer Vision and Pattern Recognition (CVPR)*, vol. 1. IEEE, 2005, pp. 886–893.
  - [79] P. Carcagnì, M. Del Coco, M. Leo, and C. Distanto, “Facial expression recognition and histograms of oriented gradients: a comprehensive study,” *SpringerPlus*, vol. 4, no. 1, pp. 1–25, 2015.
  - [80] S. Kaltwang, S. Todorovic, and M. Pantic, “Latent trees for estimating intensity of facial action units,” in *IEEE Conference on Computer Vision and Pattern Recognition (CVPR)*, 2015, pp. 296–304.
  - [81] S. Mohseni, N. Zarei, and S. Ramazani, “Facial expression recognition using anatomy based facial graph,” in *IEEE International Conference on Systems, Man, and Cybernetics (SMC)*. IEEE, 2014, pp. 3715–3719.
  - [82] A. K. Hassan and S. N. Mohammed, “A novel facial emotion recognition scheme based on graph mining,” *Defence Technology*, vol. 16, no. 5, pp. 1062–1072, 2020.
  - [83] Y.-J. Liu, J.-K. Zhang, W.-J. Yan, S.-J. Wang, G. Zhao, and X. Fu, “A main directional mean optical flow feature for spontaneous micro-expression recognition,” *IEEE Transactions on Affective Computing*, vol. 7, no. 4, pp. 299–310, 2015.
  - [84] Y. Pei and H. Zha, “3d facial expression editing based on the dynamic graph model,” in *IEEE International Conference on Multimedia and Expo (ICME)*. IEEE, 2009, pp. 1354–1357.
  - [85] I. Kotsia and I. Pitas, “Facial expression recognition in image sequences using geometric deformation features and support vector machines,” *IEEE Transactions on Image Processing*, vol. 16, no. 1, pp. 172–187, 2006.
  - [86] Z. Liu, J. Dong, C. Zhang, L. Wang, and J. Dang, “Relation modeling with graph convolutional networks for facial action unit detection,” in *International Conference on Multimedia Modeling*. Springer, 2020, pp. 489–501.
  - [87] Y.-J. Liu, B.-J. Li, and Y.-K. Lai, “Sparse mdmo: Learning a discriminative feature for spontaneous micro-expression recognition,” *IEEE Transactions on Affective Computing*, vol. 12, no. 1, pp. 254–261, 2021.
  - [88] S. Zafeiriou and I. Pitas, “Discriminant graph structures for facial expression recognition,” *IEEE Transactions on Multimedia*, vol. 10, no. 8, pp. 1528–1540, 2008.
  - [89] C. Wu, L. Chai, J. Yang, and Y. Sheng, “Facial expression recognition using convolutional neural network on graphs,” in *Chinese Control Conference (CCC)*. IEEE, 2019, pp. 7572–7576.
  - [90] M. Zhang, Y. Liang, and H. Ma, “Context-aware affective graph reasoning for emotion recognition,” in *IEEE International Conference on Multimedia and Expo (ICME)*. IEEE, 2019, pp. 151–156.
  - [91] Y. Xie, T. Chen, T. Pu, H. Wu, and L. Lin, “Adversarial graph representation adaptation for cross-domain facial expression recognition,” in *ACM International Conference on Multimedia (ACM MM)*, 2020, pp. 1255–1264.
  - [92] J. Zhou, X. Zhang, Y. Liu, and X. Lan, “Facial expression recognition using spatial-temporal semantic graph network,” in *IEEE International Conference on Image Processing (ICIP)*. IEEE, 2020, pp. 1961–1965.
  - [93] H. Chen, Y. Deng, S. Cheng, Y. Wang, D. Jiang, and H. Sahli, “Efficient spatial temporal convolutional features for audiovisual continuous affect recognition,” in *International on Audio/Visual Emotion Challenge and Workshop*, 2019, pp. 19–26.
  - [94] A. R. Rivera and O. Chae, “Spatiotemporal directional number transitional graph for dynamic texture recognition,” *IEEE Transactions on Pattern Analysis and Machine Intelligence*, vol. 37, no. 10, pp. 2146–2152, 2015.
  - [95] D. Liu, H. Zhang, and P. Zhou, “Video-based facial expression recognition using graph convolutional networks,” *arXiv preprint arXiv:2010.13386*, 2020.
  - [96] Y. Tong, W. Liao, and Q. Ji, “Facial action unit recognition by exploiting their dynamic and semantic relationships,” *IEEE Transactions on Pattern Analysis and Machine Intelligence*, vol. 29, no. 10, pp. 1683–1699, 2007.
  - [97] Y. Zhu, S. Wang, L. Yue, and Q. Ji, “Multiple-facial action unit recognition by shared feature learning and semantic relation modeling,” in *International Conference on Pattern Recognition (ICPR)*. IEEE, 2014, pp. 1663–1668.

- [98] L. Lo, H.-X. Xie, H.-H. Shuai, and W.-H. Cheng, "Mer-gcn: Micro-expression recognition based on relation modeling with graph convolutional networks," in *IEEE Conference on Multimedia Information Processing and Retrieval (MIPR)*, IEEE, 2020, pp. 79–84.
- [99] L. Lei, T. Chen, S. Li, and J. Li, "Micro-expression recognition based on facial graph representation learning and facial action unit fusion," in *Proceedings of the IEEE/CVF Conference on Computer Vision and Pattern Recognition (CVPR)*, 2021, pp. 1571–1580.
- [100] C. Corneanu, M. Madadi, and S. Escalera, "Deep structure inference network for facial action unit recognition," in *European Conference on Computer Vision (ECCV)*, 2018, pp. 298–313.
- [101] X. Niu, H. Han, S. Shan, and X. Chen, "Multi-label co-regularization for semi-supervised facial action unit recognition," in *International Conference on Neural Information Processing Systems (NeurIPS)*, vol. 32, 2019, pp. 1–11.
- [102] T. Song, L. Chen, W. Zheng, and Q. Ji, "Uncertain graph neural networks for facial action unit detection," in *AAAI Conference on Artificial Intelligence (AAAI)*, 2021, pp. 1–10.
- [103] T. Song, Z. Cui, W. Zheng, and Q. Ji, "Hybrid message passing with performance-driven structures for facial action unit detection," in *Proceedings of the IEEE/CVF Conference on Computer Vision and Pattern Recognition (CVPR)*, 2021, pp. 6267–6276.
- [104] R. Walecki, O. Rudovic, V. Pavlovic, B. Schuller, and M. Pantic, "Deep structured learning for facial expression intensity estimation," *Image and Vision Computing*, vol. 259, pp. 143–154, 2017.
- [105] L. Zhou, Q. Mao, and M. Dong, "Objective class-based micro-expression recognition through simultaneous action unit detection and feature aggregation," *arXiv preprint arXiv:2012.13148*, 2020.
- [106] W.-S. Chien, H.-C. Yang, and C.-C. Lee, "Cross corpus physiological-based emotion recognition using a learnable visual semantic graph convolutional network," in *ACM International Conference on Multimedia (ACM MM)*, 2020, pp. 2999–3006.
- [107] Z. Xu, S. Wang, and C. Wang, "Exploiting multi-emotion relations at feature and label levels for emotion tagging," in *ACM International Conference on Multimedia (ACM MM)*, 2020, pp. 2955–2963.
- [108] W. Zheng, X. Zhou, C. Zou, and L. Zhao, "Facial expression recognition using kernel canonical correlation analysis (kcca)," *IEEE Transactions on Neural Networks*, vol. 17, no. 1, pp. 233–238, 2006.
- [109] D. Derkach and F. M. Sukno, "Local shape spectrum analysis for 3d facial expression recognition," in *IEEE International Conference on Automatic Face and Gesture Recognition (FG)*, IEEE, 2017, pp. 41–47.
- [110] H. K. Meena, K. K. Sharma, and S. D. Joshi, "Facial expression recognition using the spectral graph wavelet," *IET Signal Processing*, vol. 13, no. 2, pp. 224–229, 2018.
- [111] R. Zhi, M. Flierl, Q. Ruan, and W. B. Kleijn, "Graph-preserving sparse nonnegative matrix factorization with application to facial expression recognition," *IEEE Transactions on Systems, Man, and Cybernetics, Part B (Cybernetics)*, vol. 41, no. 1, pp. 38–52, 2010.
- [112] H.-W. Kung, Y.-H. Tu, and C.-T. Hsu, "Dual subspace nonnegative graph embedding for identity-independent expression recognition," *IEEE Transactions on Information Forensics and Security*, vol. 10, no. 3, pp. 626–639, 2015.
- [113] D. G. Lowe, "Distinctive image features from scale-invariant keypoints," *International Journal of Computer Vision*, vol. 60, no. 2, pp. 91–110, 2004.
- [114] C. Liu and H. Wechsler, "Independent component analysis of gabor features for face recognition," *IEEE Transactions on Neural Networks*, vol. 14, no. 4, pp. 919–928, 2003.
- [115] Y. Liu, X. Zhang, J. Zhou, and L. Fu, "Sg-dsn: A semantic graph-based dual-stream network for facial expression recognition," *Neurocomputing*, 2021.
- [116] J. Wang, K. Sun, T. Cheng, B. Jiang, C. Deng, Y. Zhao, D. Liu, Y. Mu, M. Tan, X. Wang *et al.*, "Deep high-resolution representation learning for visual recognition," *IEEE Transactions on Pattern Analysis and Machine Intelligence*, 2020.
- [117] B. Xiao, H. Wu, and Y. Wei, "Simple baselines for human pose estimation and tracking," in *European Conference on Computer Vision (ECCV)*, 2018, pp. 466–481.
- [118] W. Li, F. Abtah, Z. Zhu, and L. Yin, "Eac-net: A region-based deep enhancing and cropping approach for facial action unit detection," in *IEEE International Conference on Automatic Face and Gesture Recognition (FG)*, IEEE, 2017, pp. 103–110.
- [119] M. J. Lyons, J. Budynek, A. Plante, and S. Akamatsu, "Classifying facial attributes using a 2-d gabor wavelet representation and discriminant analysis," in *IEEE International Conference on Automatic Face and Gesture Recognition (FG)*, IEEE, 2000, pp. 202–207.
- [120] S. Ren, K. He, R. Girshick, and J. Sun, "Faster r-cnn: towards real-time object detection with region proposal networks," *IEEE Transactions on Pattern Analysis and Machine Intelligence*, vol. 39, no. 6, pp. 1137–1149, 2016.
- [121] K. Simonyan and A. Zisserman, "Very deep convolutional networks for large-scale image recognition," *arXiv preprint arXiv:1409.1556*, 2014.
- [122] K. He, X. Zhang, S. Ren, and J. Sun, "Deep residual learning for image recognition," in *IEEE Conference on Computer Vision and Pattern Recognition (CVPR)*, 2016, pp. 770–778.
- [123] R. A. Kirsch, "Computer determination of the constituent structure of biological images," *Computers and Biomedical Research*, vol. 4, no. 3, pp. 315–328, 1971.
- [124] T. Mikolov, I. Sutskever, K. Chen, G. S. Corrado, and J. Dean, "Distributed representations of words and phrases and their compositionality," in *Advances in neural information processing systems (NeurIPS)*, 2013, pp. 3111–3119.
- [125] Y.-I. Tian, T. Kanade, and J. F. Cohn, "Recognizing action units for facial expression analysis," *IEEE Transactions on Pattern Analysis and Machine Intelligence*, vol. 23, no. 2, pp. 97–115, 2001.
- [126] Z. Qiu, T. Yao, and T. Mei, "Learning spatio-temporal representation with pseudo-3d residual networks," in *IEEE International Conference on Computer Vision (ICCV)*, 2017, pp. 5533–5541.
- [127] P. Berkes, F. Wood, and J. Pillow, "Characterizing neural dependencies with copula models," in *International Conference on Neural Information Processing Systems (NeurIPS)*, vol. 21, 2008, pp. 129–136.
- [128] K. Hara, H. Kataoka, and Y. Satoh, "Can spatiotemporal 3d cnns retrace the history of 2d cnns and imagenet?" in *IEEE Conference on Computer Vision and Pattern Recognition (CVPR)*, 2018, pp. 6546–6555.
- [129] Z. Luo, L. Liu, J. Yin, Y. Li, and Z. Wu, "Deep learning of graphs with ngram convolutional neural networks," *IEEE Transactions on Knowledge and Data Engineering*, vol. 29, no. 10, pp. 2125–2139, 2017.
- [130] Y. Li and A. Gupta, "Beyond grids: Learning graph representations for visual recognition," in *International Conference on Neural Information Processing Systems (NeurIPS)*, 2018, pp. 9245–9255.
- [131] C. Kemp and J. B. Tenenbaum, "The discovery of structural form," *National Academy of Sciences*, vol. 105, no. 31, pp. 10 687–10 692, 2008.
- [132] D. Madigan, J. York, and D. Allard, "Bayesian graphical models for discrete data," *International Statistical Review/Revue Internationale de Statistique*, pp. 215–232, 1995.
- [133] S. Chib and E. Greenberg, "Understanding the metropolis-hastings algorithm," *The american statistician*, vol. 49, no. 4, pp. 327–335, 1995.
- [134] S. Bai, J. Z. Kolter, and V. Koltun, "An empirical evaluation of generic convolutional and recurrent networks for sequence modeling," *arXiv preprint arXiv:1803.01271*, 2018.
- [135] Y. Wang, Y. Sun, Z. Liu, S. E. Sarma, M. M. Bronstein, and J. M. Solomon, "Dynamic graph cnn for learning on point clouds," *ACM Transactions On Graphics*, vol. 38, no. 5, pp. 1–12, 2019.
- [136] T. N. Kipf and M. Welling, "Semi-supervised classification with graph convolutional networks," in *International Conference on Learning Representations (ICLR)*, 2017.
- [137] D. Tran, H. Wang, L. Torresani, J. Ray, Y. LeCun, and M. Paluri, "A closer look at spatiotemporal convolutions for action recognition," in *IEEE Conference on Computer Vision and Pattern Recognition (CVPR)*, 2018, pp. 6450–6459.
- [138] T. He and X. Jin, "Image emotion distribution learning with graph convolutional networks," in *International Conference on Multimedia Retrieval (ICMR)*, 2019, pp. 382–390.
- [139] B. Li, X. Li, Z. Zhang, and F. Wu, "Spatio-temporal graph routing for skeleton-based action recognition," in *AAAI Conference on Artificial Intelligence (AAAI)*, vol. 33, no. 01, 2019, pp. 8561–8568.
- [140] M. Defferrard, X. Bresson, and P. Vandergheynst, "Convolutional neural networks on graphs with fast localized spectral filtering," in *International Conference on Neural Information Processing Systems (NeurIPS)*, 2016, pp. 3837–3845.
- [141] P. Veličković, G. Cucurull, A. Casanova, A. Romero, P. Lio, and Y. Bengio, "Graph attention networks," *arXiv preprint arXiv:1710.10903*, 2017.
- [142] Y. Zhang, S. Pal, M. Coates, and D. Ustebay, "Bayesian graph convolutional neural networks for semi-supervised classification," in *AAAI Conference on Artificial Intelligence (AAAI)*, vol. 33, no. 01, 2019, pp. 5829–5836.
- [143] Y. Li, D. Tarlow, M. Brockschmidt, and R. Zemel, "Gated graph sequence neural networks," in *International Conference on Learning Representations (ICLR)*, 2016, pp. 1–20.
- [144] N. Aifanti, C. Papachristou, and A. Delopoulos, "The mug facial expression database," in *International Workshop on Image Analysis for Multimedia Interactive Services*. IEEE, 2010, pp. 1–4.
- [145] M. J. Lyons, J. Budynek, and S. Akamatsu, "Automatic classification of single facial images," *IEEE Transactions on Pattern Analysis and Machine Intelligence*, vol. 21, no. 12, pp. 1357–1362, 1999.
- [146] T. Kanade, J. F. Cohn, and Y. Tian, "Comprehensive database for facial expression analysis," in *IEEE International Conference on Automatic Face and Gesture Recognition (FG)*. IEEE, 2000, pp. 46–53.
- [147] M. Valstar and M. Pantic, "Induced disgust, happiness and surprise: an addition to the mmi facial expression database," in *International Workshop on EMOTION: Corpora for Research on Emotion and Affect*. Paris, France, 2010, p. 65.
- [148] G. Zhao, X. Huang, M. Taini, S. Z. Li, and M. Pietikäinen, "Facial expression recognition from near-infrared videos," *Image and Vision Computing*, vol. 29, no. 9, pp. 607–619, 2011.
- [149] I. J. Goodfellow, D. Erhan, P. L. Carrier, A. Courville, M. Mirza, B. Hamner, W. Cukierski, Y. Tang, D. Thaler, D.-H. Lee *et al.*, "Challenges in representation learning: A report on three machine learning contests," *Neural Networks*, vol. 64, pp. 59–63, 2015.
- [150] A. Dhall, O. Ramana Murthy, R. Goecke, J. Joshi, and T. Gedeon, "Video and image based emotion recognition challenges in the wild: EmotiW 2015," in *ACM on International Conference on Multimodal Interaction (ICMI)*, 2015, pp. 423–426.
- [151] A. Dhall, R. Goecke, S. Ghosh, J. Joshi, J. Hoey, and T. Gedeon, "From individual to group-level emotion recognition: EmotiW 5.0," in *ACM International Conference on Multimodal Interaction (ICMI)*, 2017, pp. 524–528.
- [152] S. M. Mavadati, M. H. Mahoor, K. Bartlett, P. Trinh, and J. F. Cohn, "Disfa: A spontaneous facial action intensity database," *IEEE Transactions on Affective Computing*, vol. 4, no. 2, pp. 151–160, 2013.
- [153] L. Yin, X. Wei, Y. Sun, J. Wang, and M. J. Rosato, "A 3d facial expression

database for facial behavior research," in *International Conference on Automatic Face and Gesture Recognition (FG)*. IEEE, 2006, pp. 211–216.

- [154] X. Zhang, L. Yin, J. F. Cohn, S. Canavan, M. Reale, A. Horowitz, and P. Liu, "A high-resolution spontaneous 3d dynamic facial expression database," in *IEEE International Conference and workshops on Automatic Face and Gesture Recognition (FG)*. IEEE, 2013, pp. 1–6.
- [155] X. Zhang, L. Yin, J. F. Cohn, S. Canavan, M. Reale, A. Horowitz, P. Liu, and J. M. Girard, "Bp4d-spontaneous: a high-resolution spontaneous 3d dynamic facial expression database," *Image and Vision Computing*, vol. 32, no. 10, pp. 692–706, 2014.
- [156] G. Zhao and X. Li, "Automatic micro-expression analysis: open challenges," *Frontiers in Psychology*, vol. 10, p. 1833, 2019.
- [157] X. Li, T. Pfister, X. Huang, G. Zhao, and M. Pietikäinen, "A spontaneous micro-expression database: Inducement, collection and baseline," in *IEEE International Conference and Workshops on Automatic Face and Gesture Recognition (FG)*. IEEE, 2013, pp. 1–6.
- [158] W.-J. Yan, X. Li, S.-J. Wang, G. Zhao, Y.-J. Liu, Y.-H. Chen, and X. Fu, "Casme ii: An improved spontaneous micro-expression database and the baseline evaluation," *PloS One*, vol. 9, no. 1, p. e86041, 2014.
- [159] A. K. Davison, C. Lansley, N. Costen, K. Tan, and M. H. Yap, "Samm: A spontaneous micro-facial movement dataset," *IEEE Transactions on Affective Computing*, vol. 9, no. 1, pp. 116–129, 2018.
- [160] F. Qu, S.-J. Wang, W.-J. Yan, H. Li, S. Wu, and X. Fu, "Cas(me)<sup>2</sup> : A database for spontaneous macro-expression and micro-expression spotting and recognition," *IEEE Transactions on Affective Computing*, vol. 9, no. 4, pp. 424–436, 2018.
- [161] S. Li and W. Deng, "Reliable crowdsourcing and deep locality-preserving learning for unconstrained facial expression recognition," *IEEE Transactions on Image Processing*, vol. 28, no. 1, pp. 356–370, 2019.
- [162] R. Kosti, J. M. Alvarez, A. Recasens, and A. Lapedriza, "Context based emotion recognition using emotic dataset," *IEEE Transactions on Pattern Analysis and Machine Intelligence*, vol. 42, no. 11, pp. 2755–2766, 2019.
- [163] A. Mollahosseini, B. Hasani, and M. H. Mahoor, "Affectnet: A database for facial expression, valence, and arousal computing in the wild," *IEEE Transactions on Affective Computing*, vol. 10, no. 1, pp. 18–31, 2019.
- [164] C. Fabian Benitez-Quiroz, R. Srinivasan, and A. M. Martinez, "Emotionet: An accurate, real-time algorithm for the automatic annotation of a million facial expressions in the wild," in *IEEE Conference on Computer Vision and Pattern Recognition (CVPR)*, 2016, pp. 5562–5570.
- [165] M. F. Valstar, T. Almaev, J. M. Girard, G. McKeown, M. Mehu, L. Yin, M. Pantic, and J. F. Cohn, "Fera 2015-second facial expression recognition and analysis challenge," in *IEEE International Conference and Workshops on Automatic Face and Gesture Recognition (FG)*, vol. 6. IEEE, 2015, pp. 1–8.
- [166] W.-J. Yan, Q. Wu, Y.-J. Liu, S.-J. Wang, and X. Fu, "Casme database: a dataset of spontaneous micro-expressions collected from neutralized faces," in *IEEE International Conference and workshops on Automatic Face and Gesture Recognition (FG)*. IEEE, 2013, pp. 1–7.
- [167] R. Zhi, M. Liu, and D. Zhang, "A comprehensive survey on automatic facial action unit analysis," *The Visual Computer*, vol. 36, no. 5, pp. 1067–1093, 2020.
- [168] P. Lucey, J. F. Cohn, K. M. Prkachin, P. E. Solomon, and I. Matthews, "Painful data: The unbc-mcmaster shoulder pain expression archive database," in *IEEE International Conference on Automatic Face and Gesture Recognition (FG)*. IEEE, 2011, pp. 57–64.
- [169] J. A. M. Correa, M. K. Abadi, N. Sebe, and I. Patras, "Amigos: A dataset for affect, personality and mood research on individuals and groups," *IEEE Transactions on Affective Computing*, 2018.
- [170] R. Subramanian, J. Wache, M. K. Abadi, R. L. Vieriu, S. Winkler, and N. Sebe, "Ascertain: Emotion and personality recognition using commercial sensors," *IEEE Transactions on Affective Computing*, vol. 9, no. 2, pp. 147–160, 2016.
- [171] S. Wang, Z. Liu, S. Lv, Y. Lv, G. Wu, P. Peng, F. Chen, and X. Wang, "A natural visible and infrared facial expression database for expression recognition and emotion inference," *IEEE Transactions on Multimedia*, vol. 12, no. 7, pp. 682–691, 2010.
- [172] A. Schaefer, F. Nils, X. Sanchez, and P. Philippot, "Assessing the effectiveness of a large database of emotion-eliciting films: A new tool for emotion researchers," *Cognition and Emotion*, vol. 24, no. 7, pp. 1153–1172, 2010.
- [173] E. A. Haggard and K. S. Isaacs, "Micromomentary facial expressions as indicators of ego mechanisms in psychotherapy," in *Methods of Research in Psychotherapy*. Springer, 1966, pp. 154–165.
- [174] P. Ekman and W. V. Friesen, "Nonverbal leakage and clues to deception," *Psychiatry*, vol. 32, no. 1, pp. 88–106, 1969.
- [175] M. Behzad, N. Vo, X. Li, and G. Zhao, "Landmarks-assisted collaborative deep framework for automatic 4d facial expression recognition," in *IEEE International Conference on Automatic Face and Gesture Recognition (FG)*. IEEE, 2020, pp. 1–5.
- [176] D. Kollias and S. Zafeiriou, "Expression, affect, action unit recognition: Aff-wild2, multi-task learning and arcface," *arXiv preprint arXiv:1910.04855*, 2019.
- [177] D. Kollias, A. Schulz, E. Hajiyeve, and S. Zafeiriou, "Analysing affective behavior in the first abaw 2020 competition," in *IEEE International Conference on Automatic Face and Gesture Recognition (FG)*. IEEE Computer Society, 2020, pp. 794–800.
- [178] X. Huang, A. Dhall, R. Goecke, M. Pietikäinen, and G. Zhao, "Multimodal framework for analyzing the affect of a group of people," *IEEE Transactions on Multimedia*, vol. 20, no. 10, pp. 2706–2721, 2018.



**Yang Liu** is currently pursuing a Ph.D. degree at the South China University of Technology, Guangzhou, China. He is a visiting scholar at the Center for Machine Vision and Signal Analysis, University of Oulu, Finland. His current research interests include facial expression recognition, affective computing, and deep learning.



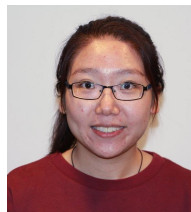
**Xingming Zhang** is currently a Professor with the School of Computer Science and Engineering, South China University of Technology, Guangzhou, China. He is a member of the Standing Committee of the Education Specialized Committee of China Computer Federation and the Standing director of the University Computer Education Research Association of China. His research focuses on video processing, big data, video surveillance, and face recognition.



**Jinzhao Zhou** received his M.S. degree in computer technology from the South China University of Technology, in 2021. He is currently pursuing a Ph.D. at the University of Technology Sydney, Australia. His research interests include affective computing, reinforcement learning, and machine learning.



**Xin Li** received the M.S. degree in computer science and engineering from the South China University of Technology, in 2021. He is currently pursuing his Ph.D. at the Department of Electrical and Computer Engineering, Rutgers University, United States. His research interests include mobile computing and sensing.



**Yante Li** received her M.S. degree in computer science and engineering from the China University of Petroleum (East China), China, in 2017. She is currently pursuing a Ph.D. degree with the University of Oulu, Finland. Her current research interests include micro-expression analysis and facial action unit detection.



**Guoying Zhao (Senior Member, IEEE)** is currently an Academy Professor with the University of Oulu, IAPR Fellow, and AAIA Fellow. She has authored or co-authored more than 260 papers in journals and conferences with 16090+ citations in Google Scholar and h-index 58. She is a co-program chair for ICMI 2021, has served as area chair for several conferences, and is an associate editor for *Pattern Recognition*, *IEEE TCSVT*, and *Image and Vision Computing Journals*. Her current research interests include image and video descriptors, facial-expression and micro-expression recognition, emotional gesture analysis, affective computing, and biometrics.